Title
Adverse, Transgenerational Effects of Prenatal Ethanol Exposure on the Epigenome, Gene Expression, Connectivity, and Behavior

Permalink
https://escholarship.org/uc/item/6st6q7p2

Author
Abbott, Charles Wilbur

Publication Date
2015

Peer reviewed|Thesis/dissertation

UNIVERSITY OF CALIFORNIA
RIVERSIDE

Adverse, Transgenerational Effects of Prenatal Ethanol Exposure on
the Epigenome, Gene Expression, Connectivity, and Behavior

A Dissertation submitted in partial satisfaction
of the requirements for the degree of

Doctor of Philosophy

in

Neuroscience

by

Charles Wilbur Abbott III

December 2015

Dissertation Committee:
        Dr. Kelly J. Huffman, Chairperson
        Dr. Peter Hickmott
        Dr. Todd Fiacco

The Dissertation of Charles Wilbur Abbott III is approved:

_____

_____

_____

                                                    Committee Chairperson

University of California, Riverside

Acknowledgements

I would like to start by thanking my mentor and friend Dr. Kelly Huffman for the wonderful experience I have enjoyed in her lab over the last five years. Dr. Huffman has been an incredible mentor, pushing me when necessary while also allowing me the leeway to explore my own ideas and press forward with new experiments. Her input and guidance have been critical for my development as a scientist, with her help I have grown immensely in my ability to approach scientific questions and work through answering them. On a personal level, Dr. Huffman has been a wonderful, caring friend. It was truly comforting knowing that if ever I needed anything she would be there for me. I will keep these happy memories with me forever.

My guidance committee members, Dr. Peter Hickmott and Dr. Todd Fiacco, have made many thoughtful and helpful contributions to my growth over the years. The thought-provoking questions and friendly conversations we had really opened my eyes, facilitating my intellectual and personal growth. I will be forever thankful for their time and input.

To my mother, father and stepfather Richard: Thank you from the bottom of my heart! Without the love and support my family I would not have made it to where I

am today. You have instilled in me a desire for knowledge and personal growth that has helped me to excel personally and professionally. I love you all!

Lastly, I would like to thank my wonderful girlfriend Jennie. She has been by my side for all of the ups and downs, bearing more burden of my stress than was fair to ask. Her day to day support helped keep me sane. Thank you so very much, I love you!

ABSTRACT OF THE DISSERTATION

Adverse, Transgenerational Effects of Prenatal Ethanol Exposure on
the Epigenome, Gene Expression, Connectivity, and Behavior.

by

Charles Wilbur Abbott III

Doctor of Philosophy, Graduate Program in Neuroscience
University of California, Riverside, December 2015
Dr. Kelly J. Huffman, Chairperson

Fetal Alcohol Spectrum Disorders (FASD) represent a wide range of

developmental conditions caused by *in utero* ethanol exposure. Today, FASD

affects nearly 1% of the total population, a number likely to be underestimated.

Cognitive, perceptual and behavioral deficits following prenatal ethanol exposure

arise from underlying neurobiological damage in developing brain structures,

including the neocortex, which is involved in higher level cognitive and behavioral

function. Current research indicates that alcohol-mediated alterations to

epigenetic function could underlie some aspects of FASD, and that these

changes may be heritable (Govorko et al., 2012; Bekdash et al., 2013). To

determine the impact of prenatal ethanol exposure (PrEE) on functional

organization of the neocortex, we first generated an FASD mouse model in CD-1

mice. Preliminary work with this model demonstrated a correlation between gross

anatomical changes, and altered gene expression patterns of RZRβ, Cad8 and

Id2 at birth along with extensive disruption in neocortical targeting within the neocortex of PrEE offspring (El Shawa et al., 2013; Abbott et al., in review). We extend these findings transgenerationally, identifying numerous stable modifications transmitted via the male germline to unexposed offspring including significant upregulation of RZRβ and Id2, as well as downregulated ephrin A5 expression in cortex. Associated with this change was a significant decrease in global DNA methylation levels in cortex. Absolute methylation levels of CpG islands in promoter regions of RZRβ and Id2 revealed significant hypomethylation in PrEE mice and their offspring. These assays established a strong inverse correlation between gene expression and DNA hypomethylation. Expression of DNMTs 1, 3A and 3B was suppressed in PrEE cortex, providing further insight into possible points at which ethanol perturbs DNA methylation, ultimately resulting in altered gene transcription. The anatomical and behavioral phenotype described in the first generation PrEE mice were also observed in the subsequent generations. These alterations in brain development could be responsible for cognitive, sensorimotor and behavioral deficits seen in our model and children with FASD and may generate phenotypes in the offspring of exposed humans. Thus, understanding the epigenetic means by which this phenotype is generated may reveal novel targets for therapeutic intervention of FASD.

Table of Contents

General Introduction

Fetal alcohol spectrum disorders (FASD) is an umbrella term used to describe a broad range of physical, neurobehavioral, and cognitive irregularities arising from *in utero* alcohol exposure. The fetal alcohol spectrum disorders can be subdivided into several diagnostic groups including pFAS (partial FAS), Alcohol-Related Neurodevelopmental Disorder (ARND) and FAS (Fetal Alcohol Syndrome) (Chudley et al., 2005). Phenotypic markers of FAS include CNS dysfunction, growth deficiency, and each of the three highly stereotyped facial abnormalities: a thin upper lip, smooth philtrum and short palpebral fissure length. The less severe classification of pFAS is used for children possessing CNS dysfunction and two out of three craniofacial abnormalities, while ARND diagnoses are reserved for individuals expressing CNS dysfunction without growth deficiencies or facial abnormalities. Exposure rates that may produce profound FAS-level effects in one individual may produce little or no effect in another. To determine what maternal characteristics are correlated with this variability, researchers have documented the effect of maternal gravidity, parity, BMI, diet, and age amongst numerous other measures. Findings have indicated that increased maternal age, gravidity and low BMI are all positively correlated with increased severity of FASD symptoms in offspring (May et al., 1983; Jacobson et al., 1996; May and Gossage, 2011). Complimenting these findings, nutritional studies have revealed that insufficient dietary intake of zinc, B12,

niacin, calcium, riboflavin, choline, folate and other methyl group donors can also increase the damage inflicted via maternal alcohol consumption (Institute of Medicine, and National Academy of Sciences USA, 1998; May et al., 2004; Tamura et al., 2004; Jensen et al., 2007). While these findings have proven fruitful in combating the effects of ethanol exposure, both individual physiological subtleties and consumption patterns amongst specific subpopulations require further attention to develop directed treatment programs.

Behavioral manifestations of FASD are a consequence of altered neurodevelopment and vary widely among affected individuals not exhibiting physical indications. Such children may exhibit hyperactivity, attention, memory and behavioral problems, difficulty with judgment and reasoning, and learning disabilities (www.nofas.org), and may have impaired brain function that leads to delayed motor development, poor coordination and somatosensory function resulting in diminished motor skill performance, and increased reaction time and response latency (Streissguth et al., 1984; Lopez-Tejero et al., 1986; Carmichael-Olsen et al., 1998; Burd et al., 2003; Connor et al., 2006). Children diagnosed with FASD will also frequently exhibit attention deficits, impaired sociability, reduced learning and memory, and a significant increase in symptoms of anxiety and depression (Mattson and Riley, 1998). These cognitive and behavioral changes are correlated with a number of neocortical abnormalities including

delayed P300 spike firing in the parietal cortex and abnormal activation of

dorsolateral prefrontal cortex during working memory tasks (Kaneko, 1996a, b;

Connor and Mahurin, 2001). Additionally, recent work from our laboratory has

demonstrated a correlation between deficits in sensorimotor integration, ectopic

intraneocortical (INC) projections and disrupted gene expression within the

neocortex following prenatal exposure to ethanol (El Shawa et al., 2013).

The Neocortex and FASD

During development, the cerebral cortex arises from the most anterior portion of

the neural plate of the embryonic ectoderm, eventually developing into three

distinct regions: the neocortex, archicortex and paleocortex. The neocortex, a

radial-layered structure with each of its six layers exhibiting distinct connectional

and functional properties, is a complexly organized brain structure responsible for

integration of the senses, language, cognition, emotion, and precise motor

control, abilities that are sometimes disrupted in humans with FASD. Laminar

organization of the neocortex is patterned into six radially organized strata.

Tangentially, the neocortex undergoes developmental division into functionally

distinct areas through a process termed arealization (O'leary, 1989; O'leary and

Sahara, 2008; Rakic, 1988; Rash and Grove, 2006; Sur and Rubenstein, 2005).

The resulting areas of unique cyto- and chemoarchitecture provide a foundation

for the emergence of an intricate neural network comprised of tightly organized

intraneocortical connections (INCs), the development of which is thought to be regulated by specific cortical gene expression patterns (Huffman et al., 2004; Dye et al., 2011a; 2011b). Appropriate areal patterning of neocortex is critical to normal development, and disruption of organizational mechanisms, including epigenetic modification from something like maternal ethanol consumption during pregnancy, can result in developmental disorders where higher-order processes are severely impaired (Beckmann, 1999; Gillberg, 1999; Dawson et al., 2005; Pardo et al., 2005; Johansson et al., 2006; Nagarajan, 2006).

Early forebrain development and patterning

During embryogenesis, the developing nervous system relies of molecular signals to identify rostral vs. caudal and dorsal vs. ventral. Patterning centers within specific rostral, caudal, dorsal or ventral locations secrete signaling molecules including Fgf8, Wnt, Bmps and Shh that impart positional information and direct regional growth of the brain (Shimamura and Rubenstein, 1997; Rubenstein et al., 1999; Ragsdale and Grove, 2001; O'Leary and Nakagawa, 2002; Ohkubo et al., 2002; Assimacopoulos et al., 2003; Garel et al., 2003; Grove and Fukuchi-Shimogori, 2003). Current research suggests intrinsic regulation of early forebrain patterning by three patterning centers. Fgf8, secreted by the rostral patterning center (RPC) interacts with Shh expressed by a ventral patterning center (VPC) and the dorsal patterning center (DPC), which expresses Wnts and BMPs (Shimamura and Rubenstein, 1997; Crossley et al., 2001;

4

Shimogori et al., 2004; Sur and Rubenstein, 2005; Storm et al., 2006).

Neocortical development and patterning

After polarization of the developing forebrain, the process through which the cortex is subdivided into specialized primary sensory and motor areas is referred to as neocortical arealization. The mechanisms underlying arealization have been a topic of debate over the past 25 years. In a now classic model of neocortical development, Rakic (1988) outlined his Protomap Hypothesis, which suggested that cortical areas are specified early in development by molecules within the proliferative zone of the neuroepithelium. Initial data supporting the protomap theory suggest that early cortical patterning is achieved through the complex interaction of both cellular and molecular mechanisms (reviewed by: Grove and Fukuchi-Shimogori, 2003; Sur and Rubenstein, 2005; Mallamaci and Stoykova, 2006; Rash and Grove, 2006; O'Leary, Chou and Sahara, 2007; O'Leary and Sahara, 2008; Hoch et al., 2009), including the expression of a coarsely graded areal pattern within the emergent cortical plate and cortical progenitor zone (Nakagawa et al., 1999; Rubenstein et al., 1999). Since Rakic first proposed his idea, scientists have reached a consensus that the 'molecular mechanisms' involved in neocortical patterning is graded or regional gene expression. Studies that highlight ways that gene expression contributes to developmental patterning provide support for the Protomap Hypothesis (Rakic,

1989) and suggest that intrinsic signals within developing cortex do regulate key features of arealization. At first this was thought to occur via thalamic input with the notion being that the expression patterns of certain genes played attractive axon targeting roles. Thus, it was thought that graded gene expressed provided a guidance cue for thalamocortical afferents. However, research from the Rubenstein laboratory, using a Gbx2 gene knock out mouse, demonstrated that thalamic input was not necessary for proper establishment or maintenance of areal gene expression or intraneocortical connections, further affirming the predominant role of intrinsic patterning mechanisms in early regionalization of the cortex during embryogenesis (Miyashita-Lin et al., 1999; Nakagawa et al., 1999, Huffman et al., 2004).

Despite a wealth of data supporting the Protomap hypothesis, the current consensus is that activity-dependent mechanisms, such an input from the sensory registers, plays an equally important role in arealization. This model, established through ablation and transplantation research, is referred to as the Protocortex Hypothesis. This model, first described by Dennis O'Leary in 1989, suggests that thalamocortical afferent input is required for the generation of area-specific cytoarchitecture and function (Wise and Jones, 1978; Dehay et al., 1991; Olearly et al 1989; Rakic et al., 1991; Schlaggar and O'Leary, 1991; Gitton et al., 1999). To address these complexities, a broad range of research has been

conducted using a variety of approaches in an attempt to the resolve the Protomap vs. Protocortex debate and the current consensus in the field of developmental neuroscience is that neocortical arealization results from an interaction of intrinsic, activity-independent (Protomap) and extrinsic, activity-dependent (Protocortex) mechanisms. This dissertation examines how a toxin (ethanol) can alter intrinsic patterning in cortex via disruption in gene expression.

Gene expression and it's role in neocortical patterning

As described above, the process of arealization is driven initially by graded expression of several known genes, including COUP-TFI, which in turn regulate expression of other transcription factors (Id2, RZRβ and Tbr1), cell adhesion molecules (Cad6 and Cad8) and axonal guidance molecules (EphrinA5), confining expression into both regional, and layer specific patterns (Miyashita-Lin et al., 1999; Bishop et al., 2000, 2002; Mallamaci et al. 2000; Zhou et al., 2001). Consequently, secretion of these molecules could be involved in the broad regulation of axon-axon connections as well as intraneocortical, thalamocortical, and corticothalamic connectivity. Below we will discuss the developmental relevance of key genes acting downstream from patterned gene expression established during regionalization.

COUP-TFI: COUP-TFI is an orphan nuclear receptor expressed by both

progenitors and CP neurons in a bi-directional gradient: high posterior-lateral to low anterior-medial. By manipulating these gradients with either loss-of-function or gain-of-function mutants, researchers gathered evidence suggesting a coordinating role for COUP-TFI in cortical patterning, laminar fate, and neurogenesis via the modulation of MAPK/ERK, AKT and beta-catenin signaling (Faedo et al., 2008). In gain-of-function experiments, increased COUP-TFI expression within rostral and dorsal cortical progenitor cells organized caudal and ventral fates, respectively, while also suppressing the number of progenitor cells and increasing early-born neurons. Cortical deletion of COUP-TFI resulted in significant compression of sensory areas and an expansion of frontal areas, which proceed to overtake most of the neocortex (Armentano et al., 2007; Faedo et al., 2008). Together, these findings suggest COUP-TFI expression is central to the regulation of regional specification through the repression of frontal/motor area identities, the specification of sensory area identities, and the guidance of cell proliferation and differentiation. The far-reaching effect of COUP-TFI in regionalization makes it an attractive target for study in our PrEE model, as alterations here could be responsible for a large number of effects.

Id2: Id2 is part of a family of genes involved in the regulation of cellular differentiation via the negative control of helix-loop-helix genes (Kadesch et al., 1993). Id2 exhibits high levels of expression in layer V of the caudal neocortex,

complimentary to that of Tbr1, which is highly expressed in the rostral neocortex (Bulfone et al., 1995). Building on these findings, a battery of anatomical assays identifying known areal boundaries was conducted. Data from cytochrome oxidase staining (CO), immunoreactivity for serotonin, and Nissl staining were compared to Id2 expression, and demonstrated that layer 5 Id2 expression marks the transition from sensory to motor areas (Rubenstein et al., 1999). Preliminary research by our laboratory with PrEE mice has demonstrated an expansion of layer III/IV Id2 expression in parietal cortex, an area showing correlative dysregulation of INC projections (See preliminary data below).

Cad8: Cadherin 8 (Cad8) is a member of a classic type-II cell-cell adhesion family, functioning via a selective homophilic interaction, joining cells expressing similar Cad proteins (Suzuki et al., 1991; Murphy-Erdosh et al., 1995). In the developing neocortex, a number of different cadherins are regionally expressed, delineating areal boundaries (Redies, 1995; Redies and Takeichi, 1996). The cadherin-associated proteins β-catenin and αN-catenin are localized within the synaptic junction of many neurons, forming symmetrical adhesion structures that link presynaptic and postsynaptic membranes (Uchida et al., 1996). This pattern of localization, combined with the finding that the cortex exhibits area-specific expression patterns of different cadherins with the same cadherins expressed in the associated thalamic nuclei suggest a role in the selective association of

9

neurons and network formation, with Cad8 performing this function within the visual cortex (Suzuki et al., 1997). Preliminary data generated by our lab suggests ethanol exposure *in utero* could interfere with proper expression of Cad8, as indicated by the lateral expansion of the Cad8 expression domain observed in PrEE mice (see preliminary data below).

Lhx2: The expression of the Lhx class of Lim homeodomain proteins has been implicated in the control of cortical hem development. Shaped by Bmp2 and Bmp4 expression in the roof plate at E12.5, Lhx2 is excluded from the cortical hem, showing expression in a high-to-low posterior-medial to anterior-lateral gradient within the cortical ventricular zone (Monuki et al., 2001). Knockout studies eliminating the substantial expression of Lhx2 at this developmental time point (E12.5) causes premature cessation of proliferation and a dramatic reduction of size in the neocortex, with a commissural expansion of the hem, suggesting that Lhx2 is critical to proper boundary formation between the hem and cortical ventricular zone, in addition to guiding their fates (Porter et al., 1997; Bulchand et al., 2001; Monuki et al., 2001). Multiple experiments in work by Mangale et al. (2008) with conditional Lhx2 knockout mice, which sidestep the lethality encountered in traditional knockout mice, further defined two primary roles for Lhx2 in development. Firstly, Lhx2 functions as a selector gene during an early critical period, working cell-autonomously to specify cortical identity while

suppressing the medial fate of the cortical hem and the lateral fate of the

antihem. Secondly, by cloning and embedding Lhx2$^{-/-}$ cells into a wild type cortex

Mangale et al. were able to demonstrate a role as a hippocampal organizer

(Mangale et al., 2008). Numerous irregularities have been reported in hippocampi

of animals exposed to ethanol prenatally, some of which suggest genetic

regulation may be impaired (Patten et al., 2013; Tunc-Ozcan et al., 2013). As

such, the influence of PrEE on Lhx2 expression is of considerable interest.

RZRβ: RZRβ is an orphan nuclear receptor related to retinoid and thyroid

hormone receptors, with high levels of expression in layer IV of the cerebral

cortex (Schaeren-Wiemers et al., 1997). Recent work by Jabaudon et al. (2013)

has demonstrated a functional role for RZRβ in regulation of areal patterning

during cortical development. Employing immunocytochemistry techniques, they

were able to demonstrate a progressive increase in RZRβ expression by neurons

in layer IV of the somatosensory cortex during barrel formation. Additionally, by

stimulating overexpression of RZRβ during development of the cortex, Jabaudon

et al. were able induce periodic clustering of neurons into structures with

characteristics similar to that of barrels receiving thalamocortical input. From

these data the authors suggest that RZRβ contributes to cytoarchitectonic

patterning of layer IV neurons into barrels within the somatosensory cortex both

via a cell-intrinsic mechanism, and, possibly through activity-dependent

regulation of expression by TCAs (Jabaudon et al., 2013). Recent work in our laboratory has demonstrated a dramatic shift in RZRβ expression in both rostral and caudal parietal cortices of PrEE mice. The lateral cortical expansion in response to ethanol observed could possibly underlie sensorimotor deficits we report at P20 (see preliminary data below).

Ephrin-A5: Ephrin-A5 is a ligand associated with the Eph family of receptor tyrosine kinases, which has been shown to, as a whole, serve as topographic labels in numerous extra- and intracortical circuits within the brain (O'Leary and Wilkinson, 1999; Bolz et al., 2004; Pasquale, 2005; Egea and Klein, 2007). Ephrin A5 in particular can function as a repulsive cue within the thalamocortical system acting on projections from the ventral posterior (VP) nuclei of the thalamus destined for S1. Co-mutual gradients of EphA4 in the VP and Ephrin A5 in S1 underlie intra-areal organization/topography of S1 via an expression level homogeny paradigm: areas of high EphA4 in the VP will form connections with areas of high Ephrin A5 expression in S1, whereas areas of low EphA4 will form connections with areas of low Ephrin A5 expression (Vanderhaeghen et al., 2000; Yun et al., 2003). Ephrin A5 also contributes to interareal topography through graded expression in the telencephalon, which guides projections of specific thalamic nuclei to the proper cortical area (Dufour, 2003). Evidence has also been generated for Ephrin A5 that suggests it also functions as an attractive

cue. Initial experiments demonstrated that layer VI axon collateral formation could be induced by Ephrin A5 expression, with later experiments showing that it could also induce collateral formation in TCAs, promoting terminal thalamocortical arborization in layer IV (Castellani et al., 1998; Mann et al., 2002; Uziel et al., 2008). In 2013 Sheleg et al. demonstrated an interesting link between ephrin-A5 deficiency and altered sensorimotor and monoaminiergic development. Using a knockout mouse model, they demonstrated through an extensive battery of sensorimotor tests and western immunoblotting that Ephrin A5 null mutants exhibited significantly increased motor activity in both social and non-social conditions, developmental delays and decreased regional levels of monoamines, similar to that seen in individuals diagnosed with certain developmental disorders (Sheleg et al., 2013). The critical role Ephrins play in axonal pathfinding warrants further investigation into their possible function in the extensive aberrant INC projections in PrEE mice recently reported by our laboratory (see preliminary data below).

Epigenetic modification and FASD

Epigenetics is a term used to describe heritable changes in gene expression that are not caused by changes in DNA sequence, but rather how the sequence is read. DNA methylation and histone modification (Figure 1), two types of epigenetic modification, regulate a number of critical developmental events

including stem cell maintenance, germ cell imprinting, cell fate, and tissue

patterning (Bartolomei, 2003; Cheng et al., 2005; Kiefer, 2007; Meshorer, 2007;

Surani et al., 2007). Epigenetic modifications have a broad range of effects: they

act to regulate the expression of individual genes, thereby shaping

developmental patterns; they underlie tissue specific changes; and they play a

role in the maintenance of cellular memory, contributing to developmental

stability (Cavalli, 2006; Kiefer, 2007). Furthermore, numerous developmental

disorders including autism, Rett Syndrome and Fragile X syndrome are

associated with atypical epigenetic modification in response to aversive

environmental stimuli (Zhao et al., 2007).

DNA methylation, which modulates gene expression and chromosomal structure,

is the most widely studied epigenetic modification (Miranda and Jones, 2007).

Methylation is accomplished through the activity of DNA methyltransferase

(DNMT), which facilitates covalent addition of a methyl group from S-adenosyl-L-

methionine (SAMe) to the fifth carbon position of cytosine bases that are followed

by guanine (CpG dinucleotide), usually contributing to gene silencing (Smith et

al., 1992). Methylation of the cytosine residue of the CpG dinucleotide is critically

important in X-chromosome inactivation, embryogenesis, and genomic imprinting

(Kafri et al., 1992; Riggs and Pfeifer, 1992; Falls et al., 1999; Kiefer, 2007). Areas

densely populated with groups of CpG repeats are termed CpG islands and are

generally located in the promoter region of the 5' flanking region of numerous

tissue-specific genes, these repeats act as the substrate for DNA methylation

(Bird et al., 1987; Gardiner-Garden and Frommer, 1987; Larsen et al., 1992;

Takai and Jones, 2002). Methylation status of CpG dinucleotides, which

contributes directly to the expression level of the target sequence, serves as a

site of teratogenic action by ethanol. Here, ethanol causes inhibition of folate-

mediated methionine synthesis, thereby disrupting s-adenosyl methionine

mediated methylation via an inhibition of methionine synthase and methionine

adenosyl transferase (Mason and Choi, 2005). These changes affect numerous

methyl donor groups and generate long-lasting alterations to DNA methylation

profiles and downstream gene expression patterns (Mason and Choi, 2005;

Green et al., 2007; Haycock and Ramsay, 2009; Liu et al., 2010; Laufer et al.,

2013).

Histone proteins assemble into a core around which DNA is wrapped, forming a

nucleosome, the basic building block of chromatin (Kornberg and Lorch, 1999).

Gene transcription is regulated, in part, by the accessibility of chromatin to

transcriptional factors and RNA polymerases, and the efficiency with which they

can bind DNA (Smith, 1991; Jenuwein and Allis, 2001). One condition underlying

this binding efficiency is the modification state of the core histone proteins (H2A,

H2B, H3 and H4), which can be altered through acetylation, methylation,

phosphorylation, and ubiquitylation, thereby changing histone-DNA and histone-

histone linking probability (van Holde, 1988; Smith, 1991; Strahl and Allis, 2000). Acetylation level, in particular, has been implicated in the regulation of gene expression, and is modulated via the enzymatic action of histone acetyltransferases (HATs) and histone deacetylases (HDACs) (Strahl and Allis, 2000; Tsankova et al., 2007; Chandramohan et al., 2008). Increasing the amount of HAT activity will acetylate lysine residues, "relaxing" the chromatin structure, permitting increased transcription factor binding to the DNA and commiserate increases in gene expression (Smith, 1991; Stahl and Allis, 2000). Conversely, HDACs remove acetyl groups, driving the condensation of chromatin, thereby reducing gene transcription (Dokmanovic and Marks, 2005; Xu et al., 2007). Adult animals exposed to a chronic prenatal ethanol exposure paradigm exhibit decreased histone activation marks including acetylation and methylation within POMC neurons of the hypothalamus (Bekdash et al., 2013). Treatment with the methyl group donor choline reverses some of the associated dysfunction, including altered gene expression and histone methylation, suggesting that chromatin remodeling is a possible mechanism by which PrEE achieves its deleterious effects (Maclennan et al., 1995; Ishii et al., 2008).

Choline supplementation and PrEE

One carbon metabolism is a biosynthetic pathway that uses folic acid as a substrate for the generation of the methyl group donor SAMe, a critical

intermediary required for a number of epigenetic mechanisms including

methylation of DNA and histone, as well as numerous physiological processes

involved in neurodevelopment in mammals (Kim et al., 2009; Robertson and

Wolffe, 2000). Proper choline levels are required for normal fetal growth and

brain development in mammals (Zeisel, 2006). Choline deficiency causes a

range of neurodevelopmental deficits including altered neuronal differentiation,

migration and survival, as well as neural tube defects (Fischer et al., 2002;

Craciunescu et al., 2003; Shaw et al., 2004; Zeisel, 2006; Zeisel, 2011).

Furthermore, choline deficiency modulates DNA and histone methylation and

gene expression in tissue-specific manner within the brain (Kovacheva et al.,

2007; Davison et al., 2009; Mehedindt et al., 2010). Two recent studies have

established a therapeutic role for dietary choline supplementation in both prenatal

and early postnatal ethanol exposure paradigms, where it attenuated some of the

detrimental effects on learning and memory (Thomas et al., 2007, 2010). One

mechanism by which choline achieves these restorative effects is through the

normalization of SAMe levels, and therefore, methylation (Olthof and Verhoef,

2005). In the presence of ethanol, folate metabolism is inhibited, which impairs

downstream transmethylation reactions and SAMe levels. This inhibition causes

a metabolic shift to choline and it's intermediary, betaine, in the generation of

methionine from homocysteine prior to the production of SAMe. Supplementation

with choline helps to meet the increased demand this creates. The requirement

of choline for proper physiological function, methylation and general neurodevelopment supports our belief that gestational choline supplementation will be an effective treatment for the attenuation of detrimental effects we have observed in our mouse model of FASD.

Furthered understanding of the mechanisms by which PrEE impacts neocortical organization is of critical importance to the fields of human health and developmental neurobiology. PrEE mediated disruptions in brain development have been characterized (Chen et al., 2003; Guerri et al., 2009; O'Leary-Moore et al., 2011), however the extent to which ethanol disrupts development has yet to be defined. By conducting a quantitative genetic and epigenetic analysis of cortical alteration in PrEE mice, and exploring dietary methods to reverse these deviations, we will accomplish two goals: identification of a new point of teratogenicity underlying the phenotype, and provide a possible dietary intervention to reverse these changes. We will examine regional expression levels of 6 genes involved in areal patterning, methylation levels of these genes and histone modification state, and assess the efficacy of treatment with choline, a methyl group donor.

Preliminary data generated by our laboratory showing a PrEE-induced shift in the development of INCs and a corollary alteration in gene expression revealed a

possible mechanism by which prenatal ethanol exposure can drive a cascade of changes culminating in the cognitive and behavioral phenotypes. By extending these findings and developing a more complete, and quantitative, profile of changes to gene expression gradients, including transcript level and epigenetic modification status we will provide novel information on how ethanol exposure impacts cortical gene expression during development, with a strong potential impact for human health.

Chapter 1: Anatomical and transcriptional changes in mouse brain following prenatal ethanol exposure.

Introduction

Fetal alcohol spectrum disorders (FASD) describe a continuum of neurological, behavioral and physical abnormalities caused by prenatal exposure to ethanol (PrEE). Humans with FASD exhibit stereotyped neurological, craniofacial, skeletal and cardiovascular deficits (Jones et al., 1973; Clarren et al., 1978). Fetal Alcohol Syndrome, or FAS, represents the most severe form of FASD where the child is significantly impaired from the exposure. Epidemiological data documenting the extent of FAS in the western world suggest an incidence rate of 0.5-3.0 cases per 1,000 births (Stratton et al., 1996). However, the rates of the *spectrum*, where all levels of exposure-related deficits are included, are believed to be much higher (Stratton et al., 1996). Despite the prevalence of FASD, how PrEE impacts brain development is not completely documented and the mechanisms that lead to altered behavior in FASD are not fully understood. Identification of brain regions susceptible to the effects of *in utero* ethanol exposure will provide critical insight that can be applied to future diagnoses and treatments in people suffering from FASD.

Groups, such as the Collaborative Initiative on Fetal Alcohol Spectrum Disorders (CIFASD), which organize multidisciplinary research from a broad group of

clinical and behavioral investigators, have put forth efforts generating significant

support for links between PrEE and anatomical irregularities in the brain.

Widespread reductions in brain volume have been identified by several groups

using human brain imaging studies (Archibald et al., 2001; Lebel et al., 2008; Li

et al., 2008; Willoughby et al., 2008; Norman et al., 2009; Lebel et al., 2011).

The neocortex, specifically the parietal, parieto-occipital, temporal and frontal

lobes, seem to be particularly affected by PrEE (Riikonen et al., 1999; Archibald

et al., 2001; Sowell et al., 2002). Cortex-specific thinning has been reported in

middle frontal, inferior occipital and paracingulate areas (Zhou et al., 2011), while

thickening has been reported in inferior parietal, anterior frontal and orbital frontal

cortex of subjects exposed prenatally to ethanol (Sowell, et al. 2002a; Sowell et

al., 2002b; Yang et al., 2011). Furthermore, MRI studies in humans have

revealed abnormalities in corpus callosum, with high variability in structural form

persisting into adulthood (Bookstein et al., 2002; 2007), reduced overall size of

basal ganglia (Mattson et al., 1996) and left-right hippocampal asymmetry

(Riikonen et al., 1999). Work in rodent models of FASD report similar, albeit

generalized, changes. For example, whole brain volume, as well as cortical

volume, surface area and thickness were reduced in PrEE animals when

compared to controls (El Shawa et al., 2013; Leigland 2013).

Although studies in rodent models of FASD have reported gross regional

volumetric changes, fine-scale cortical changes throughout development have

not been fully investigated. Thus, the current study assessed cortical as well as

subcortical abnormalities across whole brain at birth (P0). Our general

hypotheses stated that PrEE would induce sensory area-specific alterations to

developmental cortical thinning. By assessing multiple locations throughout the

brain at early development we were able to map changes in the neuroanatomy of

mice exposed to ethanol *in utero*.

Methods

Animal care

The University of California, Riverside Institutional Animal Care and Use

Committee (IACUC) approved all experimental procedures. Ten-week-old

Female CD-1 mice were bred with non-sibling males, and housed alone for the

entire gestational period following confirmation of a vaginal plug (gestational day,

GD, 0.5). Dams were weight-matched, separated into ethanol-treated and control

groups, and provided *ad libitum* access to standard mouse chow. Upon birth,

post-natal day (P) 0 mice were euthanized as described below.

Ethanol Administration

Ethanol administration and determination of blood ethanol concentration levels were carried out as described previously (El Shawa et al., 2013). Dams received either 25% EtOH in water (experimental), or an isocaloric maltodextrin solution (control). Both solutions were available *ad libitum* alongside standard mouse chow for the entirety of gestation.

Daily dam intake and gestational weight gain measurements.

Daily measures of food and liquid intake were recorded at 0900 to monitor for possible confounding nutritional variance between experimental and control dams. Dams were provided with 200g of standard lab chow on GD 0.5. Food was reweighed daily at 0900 using a standard Fisher Scientific scale, with average daily values for food intake computed from all measures across gestation (GD 0.5–19.5). Liquid (25% ethanol-in-water or an isocaloric maltodextrin in water solution) intake was measured daily using a graduated drinking bottle, with average daily values calculated from all measures across gestation (GD 0.5–19.5) and compared using t test analyses. Maternal weight gain was measured using a standard Fisher Scientific scale. Average gestational weight gain was calculated by subtracting dam starting body weight on GD 0.5 from body weight on GD19.5. Daily intake measures were recorded for 48 control dams and 54 EtOH-exposed dams.

Dam plasma osmolality measurements.

Plasma osmolality was recorded to determine if ethanol-induced dehydration, a potential confound in experimental dams, was present. Whole blood samples were taken from dams at GD 18.5 and added to ice-cold centrifuge tubes containing EDTA and centrifuged at 4°C/1100 g for 5 min, obtaining a clear supernatant. A Vapro 5520 vapor pressure osmometer (Wescor) was then used to measure blood plasma osmolality. Variation in plasma osmolality between control and ethanol-exposed dams was computed using t test analyses. 15 replicates were obtained for each treatment group.

Dam BEC measurements.

Dam blood ethanol content (BEC) was determined enzymatically. Blood samples were collected from control and ethanol-treated dams at two time points: mid- (GD 9) and late-gestation (GD 19) at 0700. 0.2 ml of whole blood was collected via cardiac puncture and mixed with 1.8 ml of 6.25% trichloroacetic acid and centrifuged for 2 min at 2000 rpm to obtain supernatant. The sample was then mixed with an alcohol reagent (A7504-39; Pointe Scientific) and absorbance measured immediately using a Nanodrop ND-1000 Spectrophotometer at 340 nm wavelength. Samples were analyzed in duplicate and compared to an alcohol standard to determine blood ethanol concentration. Untreated dams were

employed as negative controls. Variance in BEC between experimental and control dams was computed using t test analyses. n = 6 for control dams at GD9 and 19, n = 11 for GD9 EtOH-exposed and n = 12 for GD19 EtOH-exposed.

Tissue Processing

Pups from ethanol-exposed and control dams were sacrificed and brains collected at P0. Body and brain weights were recorded at each time point. Following transcardial perfusion with 0.9% saline and 4% paraformaldehyde (PFA, pH: 7.4), brains were extracted, post-fixed and cryoprotected overnight in a 4% PFA, 30% sucrose solution. Tissue was then cryosectioned at 30μM in the coronal plane and mounted onto glass slides. Sections were stained following the standard protocol for Nissl Staining and imaged using Zeiss bright field microscopy coupled with a Zeiss Axiocam linked to a PC.

Anatomical Measures

Gross dorsal views of P0 control and PrEE brains were imaged using Zeiss microscopy and imaging. For anatomical measures, regions of interest in individual tissue sections were measured across all cases using an electronic micrometer in ImageJ. Cortical thickness measures in sections stained for Nissl substance were taken along a line perpendicular to the cortical sheet extending between the most superficial portion of layer I to the deepest portion of layer VI.

These included prelimbic (PL), frontal cortex (FC), primary auditory cortex (A1), primary somatosensory cortex (S1) and primary visual cortex (V1). Corpus callosum (CC) thickness was measured from the midline region. Measures of hippocampal subfield thickness were taken in CA3. Measures of basal ganglia (BG) were limited to caudate putamen, globus pallidus, and ventral palladium. BG and dorsal lateral geniculate nucleus (dLGN) volumes were calculated from serial sections (P0 PrEE n = 14; P0 Control n = 14). See Table 1 for a list of abbreviations.

Analysis of cell packing density

Cell nuclei were counted in the PL, FC, A1, S1, V1, BG and dLGN in order to quantify cell packing density within these regions. Bright-field Z-stack images of 30µM thick coronal sections stained for Nissl were collected and analyzed using the ITCN plugin for ImageJ. An electronic ROI was first drawn over the selected region, and cell nuclei number was quantified. Volumetric measurements were made by calculating the distance between top and bottom sections of the stack, and then multiplied by ROI area (P0 PrEE n = 14; P0 Control n = 14).

In situ hybridization

Gene expression assays were conducted using non-radioactive free-floating in situ RNA hybridization. DIG-labeled RNA probes against *Cadherin 8, Id2 and*

RZRβ were used to determine patterns of expression in a minimum of 5

replicates of PrEE and control mice using established protocols previously

employed by this lab (Shimamura et al., 1994; Dye et al., 2011a, 2011b). Briefly,

hemispheres reserved for hybridization were rehydrated through a methanol

series, embedded in gelatin-albumin and sectioned in the coronal plane at 100

μm using a vibrating microtome. Following hybridization, all sections were

mounted in glycerol onto glass slides, coverslipped and imaged. In normal

development these genes have expression boundaries that correlate with

developing areal borders, and are involved in axonal guidance during

development of INCs. These data were reconstructed in a coronal section where

expression patterns of all three genes in typical control and PrEE cases were

overlaid to aid in interpretation of the in situ hybridization data (see Figure 5 E1,

E2). Gene expression within specific, highlighted regions of neocortex of control

and PrEE mice was analyzed (see Figure 6). Transcript density was measured

with ImageJ software and statistically analyzed to assess group differences.

First, raw images were converted to a binary format and adjusted to a

standardized threshold. A region of interest (ROI) was then electronically drawn

over areas of either the rostral or the caudal parietal cortex. Transcript signal

presence was then measured, and reported as area fraction of total ROI. This

technique was recently described in detail by Dye et al. (2012).

Statistical Analyses

Two sample *t*-tests assuming unequal variance were used to establish significant differences in all measures. For data displayed as percent change, mean baseline corrected control was set as 100%, with experimental measures expressed as percent variation from that mean.

Results

Dam measures

Multiple dam measures were recorded to map out the effects generated by our ethanol exposure paradigm (Figure 2). To ensure our exposure paradigm did not cause malnutrition or dehydration, which could confound our findings, measures of blood plasma osmolality were taken in addition to daily measures of food intake, liquid intake and dam weight. No significant variation was detected in daily food consumption (Figure 2A; control 5.19 ± 0.17 g/day; EtOH-exposed 4.78 ± 0.20 g/day; $P = 0.16$), though a significant reduction in weight gain over the entirety of gestation was observed (Figure 2B; control 27.63 ± 0.96 g; EtOH-exposed 24.18 ± 1.17 g; $P < 0.05$). The reduced weight gain correlated with reduced litter size in EtOH-exposed dams (Figure 2C; control 11.25 ± 0.47 pups; EtOH-exposed 9.20 ± 0.60 pups; $P < 0.05$). Liquid intake remained unchanged when comparing experimental and control dams (Figure 2D; control 6.48 ± 0.25

ml/day; EtOH-exposed 6.55 ± 0.20 ml/day; P = 0.81). Measures of blood plasma

osmolality revealed no significant variance in hydration between treatments

(Figure 2E; control 308.2 ± 1.77 mosm/kg; EtOH-exposed 309.2 ± 1.65 mosm/k;

P = 0.68).

Blood ethanol content was measured at two gestational timepoints: GD9 and

GD19. EtOH-exposed dams had, as expected, significantly elevated BEC levels

at both GD9 (Figure 2F; control 0.00 ± 0.0 mg EtOH/dl; EtOH-exposed 104.4 ±

1.21 mg EtOH/dl; $P < 0.0001$) and GD19 (Figure 2F; control 0.00 ± 0.0 mg

EtOH/dl; EtOH-exposed 135.2 ± 4.12 mg EtOH/dl; $P < 0.0001$) when compared

to controls.

Sub-neocortical measures in PrEE and control mice

Dorsal lateral geniculate nucleus

Examination of dLGN size at birth revealed a significant overall reduction in size

in PrEE mice compared to non-exposed controls (Figure 3, compare A1 with A2;

A3, control 100 ± 1.767 % and PrEE 92.99 ± 0.7395 %; $P < 0.05$).

Basal ganglia

When compared to controls, the basal ganglia in the brains of newborn PrEE mice were reduced in size (Figure 3, compare B1 with B2; B3, control 100 ± 1.894 % 88.38 ± 1.501 %; $P < 0.01$).

Hippocampus

The CA3 region of the hippocampus was significantly thinner at birth in PrEE mice when compared to age-matched controls (Figure 3, compare C1 with C2; C3, control 100 ± 5.353% and PrEE 84.38 ± 3.917 %, $P < 0.05$).

Corpus Callosum

Significant differences in midline callosal thicknesses were observed between PrEE and control brains during early development, where PrEE mice had a significantly thinner CC at P0 (Figure 3, compare D1 with D2; D3, control 100 ± 1.844 % and PrEE 91.85 ± 1.430 %, $P < 0.01$).

Regional cortical thickness differences in PrEE and control mice

Ethanol exposure throughout gestation caused significant thinning of PL (Figure 4, compare A1 with A2; A3, control 100 ± 2.711 % and PrEE 93.46 ± 1.129 %, $P < 0.05$) and auditory cortex in P0 PrEE brains, when compared to P0 control tissue (Figure 4, compare D1 with D2; D3, control 100 ± 1.433 % and PrEE 84.74

± 1.277 %, $P < 0.0001$). Significant thickening of frontal cortex (Figure 4,

compare B1 with B2; B3, control 100 ± 2.231 % and PrEE 117.1 ± 4.023 % $P <$

0.001) and somatosensory cortex (Figure 4, compare C1 with C2; C3, control

100 ± 1.412 % and PrEE 109.9 ± 1.310 %, $P < 0.0001$) was observed in PrEE

mice, when compared to controls, at P0. Visual cortex thickness was significantly

altered in P0 PrEE brains, with *in utero* ethanol exposure causing appreciable

thickening of V1 at birth (Figure 4, compare E1 with E2; E3, control 100 ± 0.8511

% and PrEE 120.0 ± 1.305 %, $P < 0.0001$), when compared to controls.

Cell packing density

To determine if altered cortical thickness observed in PrEE mice was generated

by varied total cell number or degree of compaction, cell nuclei packing density

was measured in the FC, PL, A1, S1, and V1 of PrEE mice and controls at P0

(table 2). Regional cell packing density in cortex did not significantly differ at any

of the locations measured. Thus, the varied region-specific volumetric changes in

cortical thickness are not simply caused by a change in cell packing density.

Qualitative Gene Expression

At P0, patterned gene expression within neocortex has been implicated in

neocortical development as well as arealization, with graded or regional

expression correlating with developing areal boundaries (Dye et al. 2011a). Using

in situ hybridization we investigated the effect of PrEE on three of these genes: RZRβ, Cad8 and Id2.

RZRβ: In P0 control mice, an altered RZRβ expression gradient is observed in rostral sections (through caudal frontal cortex), with a noted absence in the most medial areas (Figure 5A1 left arrow). In this same section, lateral expression is shown to be moderate (Figure 5A1 right arrow). Rostral sections of parietal cortex show very light expression medially (Figure 5B1, left black arrow) and moderate to strong expression along the lateral border of the cortex, where putative rostral somatosensory cortex is located (Figure 5B1, black right arrow). Contrasting these findings, PrEE mice exhibit greater RZRβ expression in rostral-medial cortex (compare Figure 5A2 PrEE left arrow with Figure 5A1 control left arrow). Also, the lateral expression at this level is greater in the PrEE brains compared to controls (compare Figure 5A2 PrEE right arrow with Figure 5A1 control right arrow). Additionally, a higher level of transcript in medial cortex is found in more caudal sections of the PrEE brain, in rostral parietal cortex (compare Figure 5B2 PrEE left black arrow with Figure 5B1 control left black arrow). The medial boundary of high *RZRβ* expression typically correlates with the developing medial border of somatosensory cortex in controls (see white arrow in Figure 5B1; for review see Dye et al. 2011a); this RZRβ boundary has shifted in PrEE neocortex (compare Figure 5B1 and 5B2 white arrows)

suggesting a disorganization of normal cortical development. The region of

increased RZRβ expression located laterally in PrEE brains corresponds to

somatosensory cortex and suggests a disruption of normal patterning (compare

Figure 5B2 PrEE right black arrow with Figure 5B1 control right black arrow). In

normal mice, cells projecting to visual cortex at P0 are typically within *RZRβ*

positive zones, as RZRβ expression at this age corresponds with putative visual

cortex and is anti-correlated with motor cortex (see Dye et al 2011a, for review).

In PrEE cortex, abnormal RZRβ expression within the boundaries of developing

somatosensory motor cortex correlated with an area that sends abnormal

projections to the putative visual cortex in our dye tracing studies (see El Shawa

et al., 2013 Figs. 3, 6). Atypical gene expression may generate the PrEE-related

disruption in INC development, as the two processes have been linked in a

previous report (Huffman et al. 2004). Quantification of RZRβ transcript density

within regions of interest (ROI, boxed in Figure 6A1, B1) revealed a significant

increase (P<0.001) in area fraction in PrEE mice in both rostral (Figure 6A2:

control 9.09±0.51%, PrEE 39.44±0.32%; p<0.001), and caudal (Figure 6B2:

control 7.87±0.24%, PrEE 46.01±3.32%; p<0.01) sections of the putative motor

and somatosensory cortex.

Cad8: Cadherin8 *(*Cad8) is strongly expressed in developing frontal/motor cortex

in control mice (Dye et al. 2011a). Typically, regions of strong RZRβ and Cad8

expression do not overlap in this neocortical region at P0. However, we found a

lateral extension of Cad8 expression in our PrEE cortices (compare Figure 5 C1

and C2 arrows marking the lateral edge of Cad8 expression). These patterns of

RZRβ and Cad8 expression overlap slightly in the PrEE cortex (compare Figure

5 B2 white arrow and C2 black arrow) demonstrating a disorganization of normal

patterning. The shift in Cad8 expression is also documented statistically in our

density measures, showing increased transcript in our PrEE ROI (boxed in Figure

6 C1) (Figure 6. C2, control 45.15±3.21%, PrEE 67.45 ± 2.00%; $p<0.05$).

Id2: In addition to abnormalities in RZRβ and Cad8 expression, we found some

differences in Id2 expression in PrEE neocortex. In control P0 mice, developing

cortical layers 3 and 4 are negative for Id2 expression in rostro-medial cortex

(Figure 5 D1, arrow). However, PrEE mice show an extension of the lateral *Id2*

positive zones within these layers (Figure 5 D2, arrow). The shift in Id2

expression is also documented statistically in our density measures, showing

increased transcript in our PrEE ROI (boxed in Figure 6 D1; Figure 6 D2, control

8.48±0.82%, PrEE 40.19±3.70%; $p<0.001$).

Discussion

In this report we describe structural and transcriptional abnormalities in PrEE

mice at postnatal days 0. By detailing developmental changes in the patterning

and neuroanatomy of PrEE mice, we gain a more complete understanding of

ethanol's impact on the trajectory of cortical thinning, nuclear size, structural

features and underlying gradients of gene expression during early development.

Furthermore, correlated changes to gene expression patterns in the same

animals suggests that PrEE-derived alterations to these gradients may underlie

some commonly observed cognitive and behavioral impairments observed in

children with FASD.

Extra-Neocortical brain structures altered by PrEE

Commensurate with PrEE induced changes in brain size and cortical thickness,

widespread extra-neocortical abnormalities have been detected in both mice

exposed to ethanol during gestation and children with FASD, with neuroimaging

studies revealing the largest variation residing in BG, CA3 regions of the

hippocampus and the CC (Niccols, 2007; Derauf et al., 2009; Norman et al.,

2009; Godin et al., 2011). As such, these regions, along with the dLGN, were

investigated in our model.

dLGN: Our data demonstrate a reduction in the size of dLGN in P0 PrEE mice

when compared to control. We believe this change is two-fold: the reduction in

the dLGN in the PrEE animals may result from altered expression of *ephrin A5* in

the nucleus, as its development is linked to the expression (Dye et al., 2012).

We also suggest that PrEE, in addition to disrupting other developmental programs, induces a developmental delay.

Basal Ganglia: We observed decreased volume of the PrEE BG at P0, which is consistent with reductions seen in humans. Human measures of BG volume typically corroborate this finding, revealing an overall reduction during early postnatal and adolescent periods (Mattson et al., 1996; Godin et al., 2011). Basal ganglia function has been previously implicated in motivational, cognitive and affective functions (Devinsky and D'Esposito, 2004). Our data demonstrates an increase in both anxiety-like behavior and deficits in motor function in PrEE mice at P20 (El Shawa et al., 2013), behaviors associated with BG function. This suggests that perturbations in early development may be sufficient for the generation of long-lasting behavioral consequences.

Hippocampus: Clinical investigations have established a distinct association between gestational ethanol consumption and learning and memory deficits in exposed offspring (Willford et al., 2004). Owing to this vulnerability even moderate levels of ethanol exposure during development are sufficient to reduce hippocampal CA1 and CA3 pyramidal cell number, and alter dendritic morphology. In the present report, stereological analysis of the CA3 region of hippocampus revealed a reduction in CA3 thickness at P0 in PrEE mice. It is

likely that the early reduction detected at P0 results from a combination of factors including reduced neurogenesis, synaptogenesis and decreased cell and spine density (Tarelo-Acuna et al., 2000; Livy et al., 2003; Cullen et al., 2014).

Corpus Callosum: Midline callosal hypoplasia was detected at P0, consistent with previous studies in both human and mouse that demonstrate an association between prenatal ethanol exposure and shape abnormalities with volumetric changes in the CC (Livy and Elberger, 2008; Gautam et al., 2014). Research conducted in humans with FASD suggests that alterations to the corpus callosum could be associated with deficits in executive function (Bookstein et al., 2002).

PrEE and cortical thickness

Prenatal ethanol exposure disrupts the normal cortical developmental trajectory, beginning with a significant thickening of FC, S1 and V1 and thinning of PL and A1 at P0 (Figure 4). The observation of reduced developmental cortical thinning during a time related to 'early childhood' in children and a maintained perturbation during early adulthood (Kozanian, 2015) in our model is reminiscent of variation seen in humans with FASD. For example, these changes mark an alteration to an essential developmental process thought to be broadly driven by arealization, and in particular, the refinement of neuronal networks, white matter myelination and synaptic pruning (Sowell et al., 2004; Shaw et al., 2008; Treit et

al., 2014). The process of cortical thinning, beginning in early development and carrying through to adulthood, proceeds at varying rates dependent upon brain region, with frontal and prelimbic regions thinning at lower rates in humans (Tamnes et al., 2010). The persistence of thickened FC in PrEE mice throughout early development is stereotaxically consistent with dysregulated intraneocortical connections previously reported by our laboratory (El Shawa et al., 2013). The failure to prune these aberrant connections may be involved in delayed cortical thinning, with these alterations potentially underlying the impaired coordination and increased anxiety we observed in P20 PrEE mice (El Shawa et al., 2013). Further evidence demonstrating the dysfunctional impact of inhibited FC thinning can be found in human studies which have demonstrated that FC thickness during development is increased in individuals with both attention deficit/hyperactivity disorder and FASD when compared to those suffering from FASD alone, a finding they attribute to immature brain development (Fernández-Jaén et al., 2011).

Prenatal ethanol exposure disrupts the processing of sensory input at multiple levels of the nervous system. One area altered by PrEE is the V1 cortical retinotopic map, which is the recipient of projections from the dLGN. Studies show a lack of connectional and electrophysiological refinement in response to prenatal ethanol exposure in V1 (Lantz et al., 2014). Somatosensory and auditory

information show similar multi-leveled processing deficits ranging from thalamic defects, to altered cortical pyramidal cell morphology and function (Church et al., 1997; Mooney et al., 2010; Church et al., 2012; De Giorgio and Granato, 2015). Taken together, these findings suggest that impaired higher-order cortical processing and integration of auditory, somatosensory and visual information may contribute to balance and motor control impairments in our mouse model of FASD.

Cortical thickness is influenced by a number of factors including cytoarchitecture, organization and overall cell number (Dunty et al., 2001; Miller, 1988). Analysis of cell packing density in the present study revealed no significant change amongst treatments (Table 2). This suggests that the maintenance of cortical thickness in PrEE animals occurs independently of cell packing density of specific cortical populations. Instead, it is probable that these changes occur at least partially through a comprehensive change in cell number, possibly generated via up/down regulation migration or proliferation pathways, which maintain cortical cell packing density despite altered cortical thickness.

Gene Expression

A pronounced extension of RZRβ into medial regions of cortex was observed in PrEE mice (Figure 5). Typically, RZRβ is expressed in a low caudo-lateral to high

rostral cortical gradient, regulating neuronal development in neocortex via differential expression in somatosensory cortical areas, with distinct increases in layer IV barrel cortex during barrel formation (Dye et al. 2011a). RZRβ regulates patterning via a cell-intrinsic mechanism, contributing to development of layer IV neurons into somatosensory barrels (Jabaudon et al., 2012). Altered expression of RZRβ, particularly extension of its boundary of expression, could underlie both the anatomical abnormalities observed and the impaired sensorimotor integration described by El Shawa et al (2013).

Id2 shows a similar shift in expression domain, particularly within layer 1/2 and 3/4 (Figure 5). This change is inversely complimented by a mild extension of the lateral Cad8 expression boundary in PrEE mice. Typically Id2 exhibits strong layer 2/3 expression in rostral cortex, with a rapid decline in intermediate neocortex (Bishop et al., 2002). This change in expression marks the boundary between somatosensory and motor areas. Id2 has been implicated in cell sensitization by affecting the chromatin structure of selected genes, modulating cell proliferation (García-Trevijano et al., 2013). By influencing epigenetic modification of chromatin structure Id2 can induce an open chromatin state, permitting increased transcription (García-Trevijano et al., 2013).

Changes in gene expression reported in this study may be caused by altered

DNA methylation, an epigenetic modification that cells use to mediate gene expression (Moore et al., 2013), cell differentiation, and embryonic development (Monk et al., 1987; Feng and Fan, 2009). Methylation occurs at the fifth position of cytosine and is driven by three conserved enzymes, DNA methyltransferase 1 (DNMT1), DNMT3A, and DNMT3B, which together are responsible for its deposition and maintenance, a function required for normal development (Li et al., 1992; Okano et al., 1999). Methyltransferase activity can be modified by exposure to ethanol; chronic exposure to ethanol is associated with reduced DNMT3B mRNA expression and hypermethylation in adults (Bönsch et al., 2006). Embryonic exposure to ethanol has been shown to alter DNA methylation patterns at neurulation, with increased methylation of genes on chromosome 10 and X correlating with an increase in neural tube defects (Liu et al., 2009). Furthermore, ethanol exposure impacts methyl donors (Mason and Choi, 2005), highlighting a possible mechanism by which ethanol, through methylation, can drive downstream epigenetic modifications and alter gene expression, as we have seen in this study (Haycock, 2009).

Chapter summary

We report alterations to developmental cortical thinning across functionally diverse regions of cortex, and altered development of extra-neocortical structures, with correlative alterations to gene expression. The observed group of

PrEE-induced alterations is consistent with documented human patterns of birth

defects present at early developmental stages. By extending our findings to

include patterned gene expression, we identify possible intrinsic mechanisms by

which PrEE interrupts proper cortical cytoarchitecture and development,

alterations that could underlie the anatomical phenotype presented here.

Additionally, as chromatin structure plays a critical regulatory role in transcription,

and chromatin state is partially regulated by Id2, it is possible that modification to

its expression could have far-reaching developmental effects.

Chapter Two: Transgenerational Conveyance of PrEE-Derived Cortical Dysregulation and Behavioral Impairments.

Introduction

Fetal Alcohol Spectrum Disorders (FASD) represent a wide range of adverse developmental conditions generated in response to *in utero* alcohol exposure affecting between 2 and 5% of the total population (Hoyme et al., 2005; May et al., 2014). The range of cognitive, perceptual and behavioral deficits observed following prenatal ethanol exposure are caused by underlying neurobiological damage in developing brain structures, including the neocortex, a part of the brain involved in higher level cognitive and behavioral function (El Shawa et al., 2013). Current animal models of FASD suggest that detrimental alterations generated via prenatal ethanol exposure (PrEE) are, in part, precipitated by modifications to the epigenome (Govorko et al., 2012, Laufer et al. 2013, Kleiber et al., 2014).

Epigenetic modifications including alterations to DNA methylation patterns and histone methylation/acetylation serve as a point of teratogenic interaction for ethanol during development, where it can generate permanent and widespread changes to gene expression (Renthal and Nestler, 2009; Govorko et al., 2012). Altered DNA methylation in response to PrEE has been described in distinct brain regions and cell types, including hippocampal tissue and

proopiomelanocortin (POMC) neurons of the hypothalamus and (Bekdash et al., 2013; Marjonen et al., 2015). These alterations can be meiotically heritable and thus transmitted across generations, effecting gene expression in individuals not directly exposed to ethanol (Govorko et al., 2012). These model data are supported by epidemiological studies that report transgenerational conveyance of numerous human diseases including Prader-Willi, Angelman, and Beckwith-Wiedemann syndrome (Adams, 2008). Evidence suggests alcohol-related diseases can also be transferred across generations: grandchildren descendant from maternal grandmothers who reported alcohol abuse exhibit higher rates of both major depressive disorders that are co-morbid with alcohol use disorders and FASD (Kvigne et al., 2008; Olino et al., 2008)

To determine the impact of prenatal ethanol exposure (PrEE) on functional organization of the neocortex, we first generated an FASD mouse model in the CD-1 strain. Preliminary work with this model demonstrated a correlation between sensorimotor integration deficits at postnatal day (P) 20 with aberrant targeting of motor/sensory intraneocortical connections (INCs), altered neocortical gene expression of RZRβ, Cad8 and Id2 at birth, and a prolonged disruption of cortical developmental thinning, which persisted into early adulthood (El Shawa et al., 2013; Abbott et al., in review). Here we extend those findings and present evidence that PrEE generates transgenerationally stable DNA

44

hypomethylation within the neocortex that is strongly correlated to increased expression of genes critical for proper brain development. Changes to methylation are also correlated with reduced expression of DNMT1, 3A and 3B, three methyltransferases responsible for DNA methylation. Additionally, we demonstrate a persistent alteration to intraneocortical connections (INC), with numerous atypical projections from frontal cortex in experimental mice. Behaviorally, these changes manifest themselves as transgenerationally stable reductions in sensorimotor function, as well as increased anxiety and depressive-like states.

Methods

Mouse Colony

All breeding and exploratory studies were performed in strict agreement with convention rules sanction by the Institutional Animal Care and Use Committee (IACUC) at the University of California, Riverside. CD1 mice initially acquired from Charles River Laboratories were used for all experiments. P90 female mice were matched with male breeders; upon confirmation of vaginal plug, the male was removed from cage, and the time was set as gestational day (GD) or embryonic day (E) 0.5. The time to conception ranged between 0-5 d with an average time of 3 d. Timed pregnant female mice were then matched by weight, housed independently, and separated into two groups, control and experimental.

45

The day of pup conception was viewed as P0. Pups from ethanol-treated dams were cross fostered with control dams upon birth to prevent postnatal ethanol exposure and avoid possible confounding physiological and behavioral changes of the original mom. Pups from control dams were also cross fostered to account for any changes

Dam Ethanol Administration

Experimental, ethanol-treated dams were given a 25% ethanol solution in water once the vaginal plug was detected (GD 0.5) to the day of birth (GD 19.5). Methods for generating the PrEE mouse model have been previously described (El Shawa et al. 2013). Briefly, experimental dams were provided ad libitum access to 25% ethanol in-water solution and standard mouse chow, while control dams received ad libitum access to water and standard mouse chow.

Dam measures

Daily measures of liquid and food intake were recorded to eliminate confounding nutritional variations between control and experimental groups. On GD 0.5, each pregnant dam was provided a feeding bowl with 30 g of standard mouse chow, which was reweighed, using a standard Fisher Scientific scale, and replenished to the 30 g start point at noon everyday. A graduated drinking bottle was used to

measure liquid (25% ethanol in water or water alone) intake. Gestational weight

gain of control and experimental dams was measured daily.

Dam blood ethanol concentration and plasma osmolality

Maternal blood ethanol content (BEC) resulting from self-administration of a 25%

ethanol in water solution or water only was determined enzymatically. Samples of

blood were drawn from control and ethanol-treated dams during two different

gestational time points, mid-gestation (GD 9) and late-gestation (just before live

birth, GD 19) between 0900 and 1200 h. After 0.2 mL of whole blood was

collected, it was mixed immediately with 1.8 mL of 6.25% trichloroacetic acid and

centrifuged for 2 min at 2000 rpm to obtain supernatant. The sample was then

mixed with an alcohol reagent (A7504-39; Pointe Scientific) and assayed using a

Nanodrop ND-1000 Spectrophotometer at 340nm wavelength. Samples were

analyzed in duplicate and blood ethanol concentrations were determined by

comparing experimental absorbance at 340nm to the alcohol standard. Pregnant

non-ethanol-treated dams were used as negative controls to insure proper assay

analysis. Differences in BEC between control and ethanol-treated dams were

computed using t test analyses. Also, to consider and rule out ethanol-induced

dehydration, a possible confound in experimental dams, we measured dam

plasma osmolality. At GD 18.5, whole blood samples taken from control and

ethanol-exposed dams were added to ice cold tubes and centrifuged at 4°C/1100

g for 10 min, obtaining a clear supernatant. We then used a Vapro 5520 vapor

pressure osmometer (Wescor) to measure blood plasma osmolality.

Pup measures

On the day pups were born, both experimental and control pup litter sizes were

recorded and pups were weighed individually using a Fisher Scale. Brains of

newborn pups used in gene expression studies were immediately extracted after

birth and the neocortex was removed and carefully separated into rostral and

caudal sections using a tissue matrix. We measured the body and brain weight

for control and experimental pups using a Fisher Scale. Cortical lengths were

measured using a micrometer. ANOVA was used to assess group differences.

Cell counts

Fluorescence microscopic images of control and experimental from P0 brains

injected with DiI and DiA in the putative visual and somatosensory cortices,

respectively, were used for cell counts. Only stereotaxically identical sections

were compared. ImageJ (NIH) was used to visualize each cell after images were

converted to binary format. Cells that were labeled within the cortex, upper

subplate, and intermediate zone were separated by electronically placing bins in

each area. Cells in which 50% or more of the cell body was located were added

to the bin and counted.

RT-qPCR

Total RNA from rostral and caudal regions of neocortex was isolated using the AllPrep DNA/RNA Mini Kit according to the manufacturer's protocol (Qiagen, Valencia, CA). cDNA was reverse transcribed from total RNA, and quantitative reverse transcription PCR was run in triplicate using the SensiMix one step kit (Bioline, Luckenwalde, Germany) according to the manufacturer's instructions using primers directed against ID2, RZRβ, CAD8, LHX2, EphA7, and EphrinA5. Primers used to detect changes in DNMT expression were obtained from Qiagen (Catalog numbers: DNMT1, PPM03685E; DNMT3A, PPM04769G; DNMT3B, PPM03690A). Relative quantification of RT-qPCR data was performed according to Pfaffl (Pfaffl, 2001), with changes in target gene expression normalized to beta actin. Primer pair sequences are listed in table 3.

Genomic imprinting on Id2 and RZRβ

Total DNA from rostral and caudal regions of neocortex was isolated using the AllPrep DNA/RNA Mini Kit according to the manufacturer's protocol (Qiagen, Valencia, CA), and prepared for promoter methylation analyses with the Epitect Methyl II DNA Restriction Kit (Qiagen, Valencia, CA) following manufacturer's instructions. For qPCR-based analyses of promoter methylation for Id2 and RZRβ for each sample, the following Epitect qPCR Methyl Promoter Primers

were used: Id2, catalog number EPMM102413-1A; RZRβ, catalog number

EPMM105704-1A. Percent promoter methylation for Id2 and RZRβ promoters

was calculated for each sample according to manufacturer's instructions (Qiagen,

Valencia, CA).

Global methylation and hydroxymethylation

5-mC and 5-hmC levels were measured in DNA isolated from rostral and caudal

cortex using Methylflash methylated and hydroxymethylated kits (Epigentek,

Brooklyn, NY, USA) per the manufacturer's instructions. The level of 5-mC and 5-

hmC in tissue samples are reported as the amount of methylated and

hydroxymethylated cytosine relative to the genomic content of cytosine. Briefly,

100 ng and 200 ng of DNA, for 5-mC and 5-hmC respectively, were bound to well

plates treated to have high affinity for DNA. Methylated and Hydroxymethylated

fractions of DNA were visualized using detection antibodies and absorbance

measured at 450 nm on a Victor 2 plate reader. The absolute quantification of 5-

methylcytosine (5-mC) and 5-hydroxymethylcytosine (5-hmC) was calculated

using a standard curve.

Behavioral analyses

Suok Test

There are various behavioral and cognitive deficits in both humans and

nonhuman mammals that are associated with PrEE. By using two behavioral

assays: the ledge test and the Suok test, we were able to assess sensorimotor

integration function and anxiety in adult PrEE mice. The Suok apparatus was

constructed, and testing performed in accordance with specifications published

previously (Kalueff et al., 2008; El Shawa et al. 2013). Animals were placed in the

center of a 2m long aluminum rod and allowed to explore the apparatus for 5

minutes. Any animals that fell were immediately placed back on the rod in the

same orientation. Trained researchers recorded measures of motor function

including falls and missteps, as well as measures of anxiety-like behavior:

directed exploration, grooming, latency to leave center and risk assessment.

Ledge test

After the Suok test, animals were immediately introduced to the ledge test.

Experimental procedures were outlined and performed previously (El Shawa et

al. 2013). Animals were placed on a vertically stabilized sheet of acrylic 50 cm

long by 30 cm high, with a thickness of 0.7 cm. Time to fall was measured, with a

maximum time of 60s assigned for remaining atop the apparatus for the entire

testing period, or successfully traversing the ledge and returning to the starting

position.

Rotarod

Motor ability, learning, and coordination were tested using an Accelerated Rotarod. Animals were placed on a rotating bar that accelerated from 4 – 40 rpm/min for 5-minute trials. All mice underwent 4 trials (one every 30 min), and latency to fall was measured within each session. If the animal was successful in maintaining its position on rotating rod without falling for the entire duration, a maximum score of 5 minutes was assigned. This testing paradigm evokes strong activation of the prefrontal cortex, allowing us to investigate the early phases of motor learning (Hikosaka et al., 2003; Rustay et al., 2003).

Forced swim test

The forced swim test was used to analyze depression-like behavior. The apparatus consists of a clear acrylic cylinder, 30 cm tall by 13 cm in diameter, which was filled with room-temperature water to a height of 20 cm. Mice were placed in the center of the water and were timed to swim and video recorded for 6 minutes. The first 2 minutes of swimming were considered as an adaptive period and the last 4 minutes were scored. Time spent mobile was scored. Animals that were immobile for greater periods of time signified hopeless behaviors, which are thought to be indicative of increased depression.

Results

General characteristics of ethanol-induced changes to brain and body

One-way ANOVA was used to compare the effect of F1 PrEE on pup body

weight, brain weight and cortical length across F1, F2 and F3 generations to

determine transgenerational stability of gross alterations generated by prenatal

ethanol exposure (Figure 7). Pup body weight was significantly reduced across

all generations of PrEE animals when compared to controls [F (3, 191) = 39.90, P

< 0.0001]. Post hoc comparisons with Tukey's HSD revealed that mean control

body weight was significantly different from PrEE animals and their descendants

(control, 1.765 ± 0.024g; F1, 1.516 ± 0.015g, MD = 0.249, P < 0.0001; F2, 1.479

± 0.023g, MD = 0.286, P < 0.0001; F3, 1.652 ± 0.016g, MD = 0.113, P < 0.01).

Brain weight in experimental animals was also significantly reduced across all 3

generations when compared to controls [F (3, 68) = 12.42, p < 0.0001]. Post hoc

comparisons revealed that the most significant deviations from control animals

occurred in the F1 and F3 generations (control, 0.105 ± 0.003g; F1, 0.088 ±

0.004g, MD = 0.018, P < 0.0001; F2, 0.095 ± 0.003g, MD = 0.010, P < 0.05; F3,

0.085 ± 0.004g, MD = 0.021, P < 0.0001). Additionally, reductions to cortical

length were also noted in all experimental groups [F (3, 46) = 9.024, P < 0.0001]

with the most apparent changes generated in F1 animals (control, 4.189 ±

0.087mm; F1, 3.781 ± 0.048mm, MD = 0.408, P < 0.0001; F2, 3.971 ± 0.042mm,

MD = 0.218, P < 0.05; F3, 3.909 ± 0.046mm, MD = 0.280, P < 0.05).

Dye labeling experiments

Sensory intraneocortical connections (INCs) provide the connectional framework

for sensorimotor integration in mammalian cortex. Disruption of this network has

been previously implicated in altered behavior in PrEE mice (El Shawa et al.,

2013). To determine if altered INC targeting persisted transgenerationally we

placed DiA and DiI crystals within putative S1 and V1 (Figure 8, A and A′),

respectively, of experimental and control mice. Analysis of dye labeling within

rostral cortical areas of experimental mice revealed ectopically labeled cells

arising from a DPL in putative V1 of experimental animals (Figure 8B-E), with

counts confirming a significant increase [F (3,34) = 6.022, P < 0.001]. Post hoc

analysis reported significant variance in labeled cells in all experimental groups,

when compared to controls (Figure 8F; control, 0.0 ± 0.0; F1, 55.5 ± 12.64, MD =

-55.5, P <0.01; F2, 43.0 ± 12.87, MD = -43.0, P <0.05; F3, 51.6 ± 12.1, MD = -

51.6, P <0.01). Caudal regions of visual and retrosplenial cortices contained

ectopically labeled cells arising from a dye placement location (DPL) within

putative S1 of all experimental animals, indicating a direct connection between

the two areas, a condition not present in controls (Figure 8B′-E′). Cell counts

within these areas of cortex revealed a significant increase [F (3,20) = 13.76, P <

0.0001] of labeled cells in F1, F2 and F3 generations when compared to controls (Figure 8F′; control, 0.0 ± 0.0; F1, 225.2 ± 20.79, MD = -225.2, P <0.0001; F2, 199.8 ± 41.46, MD = -199.8, P <0.001; F3, 192.2 ± 31.33, MD = -192.2, P <0.001).

Gene expression

Patterned gene expression at P0 is required for guiding arealization of the neocortex, with precise gene expression gradients conferring initial areal identity (O'Leary and Sahara, 2008). To determine the effect of PrEE on graded gene expression, and the persistence of these alterations across generations we performed quantitative reverse transcription PCR (RT-qPCR).

RT-qPCR

RNA expression levels of six developmentally critical genes; Ephrin A5, Eph A7, Cad8, Id2, Lhx2 and RZRβ was quantified for all groups in rostral and caudal areas of the cortical sheet (Figure 9). Compared to controls, ephrin A5 was significantly downregulated [$F_{(3,32)} = 32.01$, $P < 0.0001$] in caudal cortices of F2 and F3 animals, though not in F1 animals (Figure 9A). Significantly increased [$F_{(3,32)} = 176.8$, $P < 0.0001$] Id2 expression was detected in rostral cortex, with F2 and F3 animals exhibiting 34.4 and 6.7-fold increases, respectively, with no change in F1(Figure 9E). All experimental conditions displayed significant

upregulation of Id2 within caudal regions of cortex when compared to controls

(Fold increase: F1, 12.9; F2, 34.28; F3, 22.2; P < 0.0001). RZRβ expression was

significantly upregulated in rostral and caudal cortices [F (3,31) = 79.96, P <

0.0001]. Post hoc analysis revealed significantly increased expression in F1, F2

and F3 rostral cortex (Figure 9F; Fold increase: F1, 4.7; F2, 6.1; F3, 7.6; P <

0.001), while only F2 and F3 caudal cortex showed an increase in RZRβ

expression when compared to controls (Figure 9F; Fold increase: F2, 5.4; F3

11.32; P < 0.0001). PrEE did not evoke significant alterations to Eph A7, Cad8 or

Lhx2 expression in directly exposed animals, or their offspring (Figure 9B-D).

PrEE downregulates DNMT expression

DNA methyltransferases (DNMTs) are responsible for both *de novo* methylation

(DNMT3A and 3B) and continued maintenance of methylation status (DNMT1) of

DNA. We observed a significant reduction in cortical expression of DNMT1, 3A

and 3B in F1 PrEE animals (Figure 10A-C; F1: DNMT1, 0.48 ± 0.03, [F (3, 16) =

72.09, P < 0.0001]; DNMT3A, 0.46 ± 0.02, [F (3, 16) = 113.9, P < 0.0001];

DNMT3B, 0.49 ± 0.03, [F (3, 16) = 25.96, P < 0.0001]), with no significant change

persisting transgenerationally into F2 and F3 mice (Figure 10A-C; F2: DNMT1,

1.06 ± 0.05, P = 0.82; DNMT3A, 1.03 ± 0.04, P = 0.95; DNMT3B, 0.82 ± 0.09, P

= 0.13; F3: DNMT1, 1.03 ± 0.05, P = 0.97; DNMT3A, 1.02 ± 0.06, P = 0.99;

DNMT3B, 1.05 ± 0.05, P = 0.96).

DNA methylation

Methylation of C5 of cytosine, 5-methylcytosine (5mC) is thought to be
incompatible with active transcription when occurring near regulatory regions of
genes, either by directly modulate transcription factor binding or recruiting co-
repressor complexes via 5mC-binding proteins (Klose and Bird, 2006; Smith and
Meissner, 2013). Additionally 5-hydroxymethylcytosine (5hmC), an oxidized
product of 5mC, is also thought to modulate transcription and is of particular
importance during neuronal development (Szulwach et al., 2011; Mellen et al.,
2012; Bachman et al., 2014). To determine if PrEE in the F1 generation was
sufficient for the genesis of transgenerationally stable modifications to these
epigenetic marks we quantified global 5mC and 5hmC, and promoter-specific
5mC levels in the neocortex

Global 5mC and 5hmC in rostral and caudal neocortex

A colorimetric ELISA-like assay was used to quantify 5mC (%) levels in rostral
and caudal neocortex of P0 animals, revealing a significant reduction of DNA
methylation in experimental animals [$F_{(3,32)} = 14.69$, $P < 0.0001$] (Figure 11A).
The significant hypomethylation generated in response to PrEE in F1 animals
persisted into F2 and unexposed F3 animals (Figure 11A; control, 0.76 ± 0.01 %;
F1, 0.57 ± 0.05 %, MD = 0.19, $P < 0.05$; F2, 0.50 ± 0.04 %, MD = 0.27, $P < 0.01$;

F3, 0.49 ± 0.07 %, MD = 0.27, P <0.01). Measures in caudal cortex revealed a similar pattern of significant hypomethylation in experimental animals, an effect that persisted across generations (Figure 11A; control, 0.73 ± 0.02 %; F1, 0.52 ± 0.05 %, MD = 0.22, P <0.05; F2, 0.54 ± 0.04 %, MD = 0.20, P <0.05; F3, 0.42 ± 0.07 %, MD = 0.31, P <0.001).

Global hydroxymethylation (5hmC %) quantification was performed to determine the possible involvement in PrEE-related developmental dysfunction (Figure 11B). Interestingly, global hydroxymethylation analysis showed that PrEE mice had significantly higher levels of DNA methylation compared to control animals in both rostral and caudal areas of cortex [F (3,32) = 9.710, P < 0.0001], with post hoc analysis revealing that increase was limited to the F1 generation, and did not persist into later generations (Figure 11B; Rostral cortex: control, 0.073 ± 0.009 %; F1, 0.141 ± 0.01 %, MD = -0.07, P <0.01; F2, 0.105 ± 0.008 %, MD = -0.03, P = 0.23; F3, 0.104 ± 0.007 %, MD = -0.03, P <0.001; Caudal cortex: control, 0.093 ± 0.012 %; F1, 0.149 ± 0.007 %, MD = -0.06, P <0.01; F2, 0.119 ± 0.013 %, MD = -0.03, P = 0.43 ; F3, 0.118 ± 0.019 %, MD = -0.03, P = 0.43).

As expected, the ratio between hydroxymethylated and methylated DNA in both regions of cortex was disturbed in PrEE mice (Figure 11C), as well as their descendants (with a noted maintenance of control-like ratios in F2 caudal cortex).

A disproportionate change in the percentage of methylated DNA appears to be driving most of the observed variation (Figure 11C; Rostral cortex: F1, $P < 0.01$; F2, $P < 0.05$; F3, $P < 0.05$; Caudal cortex: F1, $P < 0.05$; F2, $P = 0.37$; F3, $P < 0.01$).

Analyses of promoter region methylation by MSP

RT-qPCR analysis of a panel of genes needed for proper cortical development revealed significant upregulation of Id2 and RZRβ transcription in PrEE mice and their offspring. As promoter methylation status is thought to modulate transcription we analyzed promoter region-specific methylation of these two genes. Quantification of methylation at the Id2 promoter region in samples from rostral and caudal neocortical regions revealed significant reductions in experimental animals, when compared to controls [$F (3,32) = 34.32, P < 0.0001$], an effect that persisted into unexposed F3 animals (Figure 12A; Rostral cortex: control, 0.150 ± 0.016 %; F1, 0.080 ± 0.023 %, MD = 0.07, $P < 0.01$; F2, 0.026 ± 0.005 %, MD = 0.14, $P < 0.0001$; F3, 0.030 ± 0.007 %, MD = 0.12, $P < 0.0001$; Caudal cortex: control, 0.157 ± 0.026 %; F1, 0.028 ± 0.006 %, MD = 0.13, $P < 0.0001$; F2, 0.031 ± 0.006 %, MD = 0.13, $P < 0.0001$; F3, 0.029 ± 0.008 %, MD = 0.13, $P < 0.0001$). Methylation of RZRβ promoter region followed a similar pattern of hypomethylation, with significant reductions across all experimental generations in both rostral and caudal regions of cortex (Figure 12B; Rostral

cortex: control, 0.086 ± 0.013 %; F1, 0.023 ± 0.05 %, MD = 0.06, P <0.01; F2,

0.029 ± 0.010 %, MD = 0.06, P < 0.01; F3, 0.022 ± 0.007 %, MD = 0.06, P <0.01;

Caudal cortex: control, 0.130 ± 0.018 %; F1, 0.055 ± 0.016 %, MD = 0.08, P

<0.001; F2, 0.030 ± 0.007 %, MD = 0.10, P < 0.0001; F3, 0.030 ± 0.011 %, MD =

0.10, P < 0.0001).

A Pearson correlation coefficient was calculated to determine the interaction

between promoter region methylation and RNA expression. There was a strong

negative correlation between promoter methylation and RNA expression in both

Id2 and RZRβ (Table 4).

Behavioral analyses

Sensorimotor integration, coordination, motor learning, anxiety-like and

depressive-like behaviors were measured in control, F1, F2 and F3 mice to

determine if PrEE was sufficient for the production of transgenerationally stable

phenotypic alterations.

The Accelerated Rotarod testing paradigm employed for this study allowed for

the assessment of coordination and the preliminary stages of motor learning

(Figure 13A). Two-way repeated measures ANOVA revealed significant variation

across trials [$F_{(3,90)}$ = 21.43, P < 0.0001], with Tukey's post hoc analysis

showing that the predominant source of variation was in F1 animals during trials 1 and 2 (P < 0.05 and P < 0.01, respectively).

Anxiety-like behavior, as measured by latency to leave center during testing on the Suok apparatus (Figure 13B), was significantly increased [F (3,52) = 7.30, P < 0.001] in the F1 and F2 generations, but did not persist to F3 (control, 0.95 ± 0.11s; F1, 6.57 ± 0.73s, P <0.01; F2, 6.39 ± 1.48s, P <0.001; F3, 3.88 ± 0.58s, P = 0.16). Stereotyped cephalo-caudal grooming behavior, thought to be indicative of low anxiety (Figure 13C), showed a significant decrease in all experimental animals when compared to controls [F (3,53) = 4.817, P < 0.01], suggesting increased anxiety (control, 1.57 ± 0.27; F1, 0.62 ± 0.21, P <0.05; F2, 0.63 ± 0.15, P <0.01; F3, 0.71 ± 0.19, P < 0.05). Two measures of sensorimotor integration, missteps and falls, were evaluated during the Suok test (Figure 13D and E). One-way ANOVA of the number of missteps determined that there was a significant variance between groups [F (3,52) = 5.72, P < 0.01], with all experimental animals performing notably worse than controls (control, 2.29 ± 0.32; F1, 5.54 ± 0.53, P <0.01; F2, 4.88 ± 0.66, P <0.05; F3, 4.69 ± 0.75, P < 0.05). Falls, considered to reflect a more severe loss of sensorimotor integration, were increased [F (3,53) = 5.653, P < 0.01] relative to controls in all experimental conditions (control, 0.50 ± 0.14; F1, 2.85 ± 0.61, P <0.01; F2, 2.00 ± 0.30, P <0.05; F3, 2.14 ± 0.48, P < 0.05).

61

The final measure in our behavioral battery was of depressive-like behavior, recorded as time spent immobile in the forced swim test (Figure 13F). Quantification of the results revealed significant variation [$F_{(3,37)} = 9.777$, $P < 0.0001$] between control and experimental animals. Tukey's multiple comparisons confirmed that PrEE generated significantly increased depressive-like behavior, and that it persisted transgenerationally (control, 156.7 ± 4.7s; F1, 207.4 ± 3.2s, $P < 0.001$; F2, 180.7 ± 4.5s, $P < 0.05$; F3, 202.0 ± 9.6s, $P < 0.001$).

Pearson product-moment correlations between sensorimotor, anxiety and depressive marks are presented in table 5. Significant correlations were observed between grooming and latency to leave center ($P < 0.01$), grooming and falls ($P < 0.01$), grooming and missteps ($P < 0.01$), falls and missteps ($P < 0.01$), falls and FST ($P < 0.01$), falls and Rotarod performance ($P < 0.01$), and missteps and Rotarod performance ($P = 0.05$).

Discussion

In the present study we demonstrate that prenatal ethanol exposure induces numerous transgenerationally persistent alterations including decreased body weight, brain weight and cortical length, atypical cortical connectivity, down- and upregulated RNA expression, decreased DNMT expression, global

hypomethylation and promoter-specific hypomethylation of Id2 and RZRβ.

Behavioral testing indicated that PrEE causes stable increases in anxiety- and

depressive-like behaviors, as well as reduced sensorimotor integration and fine

motor coordination across generations. The finding that maternal consumption of

ethanol during pregnancy can generate a wide array of transgenerationally stable

cortical and behavioral dysfunction, which persists via the male germline to

unexposed offspring, is both novel and compelling. These data support, and

extend transgenerationally, earlier work by this laboratory and others that

suggest disruption of proper cortical development and function via PrEE possibly

underlies the behavioral dysfunction observed in model organisms and children

with FASD (Holmes et al., 2012; El Shawa et al., 2013; Pickering et al., 2015).

INC Development

Abnormal development of intraneocortical connections (INCs) in response to

PrEE is characterized by two distinct sets of transgenerationally stable ectopic

projections: a group of cells that send projections from frontal/prelimbic cortex

toward putative visual cortex, and a second group spanning retrosplenial cortex

and visual cortex that project to putative S1. This loss of modality-specific

connectivity differs from normal developmental modulations in cortical

connectivity as these patterns of connectivity are not present at any

developmental time point in control animals (Dye et al., 2011a, b). These

changes are reminiscent of global functional changes observed in children with

FASD, which is believed to relate to reduced cognition in children with FASD in

cognitive function (Wozniak et al., 2013). The population of ectopically labeled

cells in frontal cortex correlates with a region of abnormal cortical gene

expression, altered levels and distribution of glucocorticoid receptors (current

chapter, Allan et al., 2014), and abnormal cortical thinning (Treit et al., 2014). As

this population of cells is sending aberrant projections to primary visual cortex, it

is possible that this input contributes to visual acuity deficits, compounding

recently reported dysfunctional visual cortex response patterns (Lantz et al.,

2014, 2015). Ectopically labeled cells in far caudal regions of cortex generated

from a somatosensory area DPL are found in PrEE mice and their unexposed

offspring. These aberrant projections occur in a region that undergoes numerous

other changes in response to ethanol, including alterations to the somatotopic

map and reduced dendritic spine density in pyramidal neurons (Oladehin et al.,

2007; Xie et al., 2010; De Giorgio et al., 2015). These findings are consistent with

parietal dysfunction seen in children diagnosed with FASD (Woods et al., 2015).

The persistent alterations to cortical circuitry observed in our model may govern

certain aspects of the sensorimotor deficits also reported here, and those present

in children with FASD.

Gene expression

Here we provide evidence for a transgenerational effect of PrEE on ephrin A5, Id2 and RZRβ gene expression in two regions of cortex (Figure 3). Id2, a potent transcription factor required for normal development (Park et al., 2013), and RZRβ, which functions in cytoarchitectural patterning of neocortex during development, and is critical for somatotopic mapping (Jabaudon et al., 2012), are both strongly upregulated. Ephrin A5, which is important for axonal guidance, is downregulated in caudal regions of cortex of F2 and F3 generation mice, but absent in exposed F1 animals. A similar absence was seen in rostral Id2 and caudal RZRβ expression in F1 animals, with significant upregulation in subsequent generations. It is possible that an acute effect of ethanol exposure in F1 animals is masking more long term, transgenerationally stable changes to transcription. As these genes have strong roles in guiding neocortical connectivity and patterning it is possible that altered expression levels underlie the ectopic labeling observed in rostral and caudal neocortical areas.

We observed a significant reduction of DNMT1, 3A and 3B mRNA expression in PrEE cortex when compared to controls. Inappropriate downregulation of DNMT3A and DNMT3B could generate *de novo* methylation errors at normally methylated CpG sites, which would then be erroneously copied by DNMT1, resulting in inappropriate maintenance following cell division. By multiplying this

65

across multiple rounds of cell division, it is possible that progressive global

hypomethylation could be generated. Furthermore, it is possible that initial

disruption of methyltransferase expression via PrEE plays a role in the

transgenerationally stable hypomethylation observed in PrEE mice.

DNA methylation

Global methylation is reduced in both rostral and caudal cortical regions in

response to PrEE, an effect that persists transgenerationally, while increased

hydroxymethylation is only present in rostral cortex of F1 animals. Loss of global

methylation is thought to be associated with increased differentiation potential in

stem cells during embryonic development (Hajkova et al., 2002). The ratio

between 5mc and 5hmc is perturbed via PrEE across generations. Alterations to

this ratio are thought to be involved in the balance between lineage commitment

and pluripotency (Ficz et al., 2011). The developmental health implications of this

relationship, particularly with regard to FASD, is presently unknown and will

require a greater understanding of the role of DNA hydroxymethylation at the

genomic level to move forward.

DNA methylation levels were quantified via MSP, revealing that PrEE induced

consistent hypomethylation of CpG-rich sites adjacent to the transcription start

site of Id2 and RZRβ across generations, exhibiting a strong negative correlation

with expression. Sites queried for methylation status in Id2 and RZRβ are both located close to the CCAAT box, which is required for transcriptional activation. CpG methylation upstream of the CCAAT box can effectively impede transcription factor binding to the CCAAT sequence (Deng et al., 2001). A study by Govorko et al (2012) found that PrEE generated transgenerational suppression of Pomc gene expression, which was associated with hypermethylation. These data offer further support to previous findings that suggest increased gene expression is associated with low promoter methylation (Kass et al., 1997; Capel et al., 2007). Thus, hypomethylation of these areas in PrEE animals and their offspring has the potential to drive increased expression, though further analyses of methylation/demethylation of these promoter domains will need to be conducted to determine functional implications.

Transgenerational behavioral dysfunction

In utero ethanol exposure generated sensorimotor integration deficits, and increased anxiety-like and depressive-like behaviors that persisted across generations. Moderate correlations were found between measures of anxiety and sensorimotor integration, and measures depression and sensorimotor integration. Children with FASD display numerous secondary disabilities including depression and anxiety, which are often associated with motor deficits (Hellemans et al., 2010, 2010). Children exposed to a combination of alcohol, tobacco and

marijuana prenatally exhibit a similar correlation between interhemispheric motor

coordination and anxiety/depressive symptoms (Willford et al., 2010). These

findings may suggest that deficits in sensory processing impair the ability of PrEE

mice and their offspring to adaptively respond to their environments, increasing

anxiety and depression.

Chapter summary

We provide evidence for widespread PrEE induced cortical dysfunction that is

transmitted across three generations, via the paternal germline, to offspring never

exposed to ethanol. Hypomethylation of CpG islands near the promoter regions

of RZRβ and Id2 correlated significantly with upregulated transcription of these

genes in neocortex. Abnormal INC development in rostral and caudal cortical

areas accompanies these changes. The neurobehavioral consequence of these

alterations is impaired sensorimotor integration accompanied by increases in

anxiety-like and depressive-like behaviors. The mechanisms by which these

deficits are transmitted through the paternal germline have not yet been defined,

and are the focus of current studies. The data presented here suggest that PrEE

induced alterations to DNA methylation alongside other modifications to the

epigenome could be responsible for transgenerational alterations to gene

expression. Furthermore, altered transcription, which upsets gene gradients

necessary for proper cortical development, could underlie abnormal development

of the intraneocortical network. The novel transgenerational behavioral,

anatomical, genetic and epigenetic effects of PrEE demonstrated here should be

strongly considered when assessing the long-term effects of fetal alcohol

exposure on developmental processes and behavior in humans.

General Conclusions

This dissertation presents an analysis of a broad group of developmental

changes generated in response to prenatal ethanol exposure. These alterations

persist transgenerationally, carried through the paternal germline, into unexposed

offspring. By expanding our model to include analysis of epigenetic modifications

occurring during development we have identified a novel mechanism by which

these heritable changes are generated, and maintained, following PrEE. The

identification of these novel alterations and interactions between them could open

up new lines of therapy for the treatment, and prevention of FASD.

The range of cognitive, perceptual and behavioral deficits observed following

prenatal ethanol exposure are caused by underlying neurobiological damage to

developing brain structures, including the neocortex. This structure regulates

numerous high-order operations including fine motor control and sensory

integration. Proper neocortical function and specificity is achieved through the

development of an intricate network of intraneocortical connections (INCs),

whose development is partially regulated by intrinsic cortical gene expression

(Huffman et al., 2004; Dye et al., 2011a, 2011b). The organization of INCs is

perturbed extensively following PrEE; cells from far rostral regions of cortex send

projections that terminate in putative visual cortex, possibly reflecting a defect in

occipital patterning, and cells in far caudal regions of cortex send aberrant

projections to putative somatosensory cortex (El Shawa et al., 2013). The apparent lack of navigational specificity observed does not reflect an acceleration or delay of development, rather a unique phenotype that is not observed in control animals of any age. We also detected gross changes in cortical thickness in these regions of cortex at P0, suggesting that our altered connectional phenotype could play a role in developmental cortical thinning. Indeed, MRI-based studies in children with FASD found a strong correlation between connectional abnormalities and deviations in regional cortical volume (Sowell et al., 2008; Treit et. al, 2014). The finding that these projections were grossly altered, and persist transgenerationally, suggests that modification to the underlying gradients of gene expression had likely also occurred, as deviations to patterned gene expression in cortex is well known to elicit broad changes in cortical connectivity (Huffman et al., 2004).

The panel of genes selected for study presently, while diverse in function, all play a role in cortical development. By determining both the changes to patterns of expression, via ISH, and level of transcription, via RT-qPCR, we gain a more complete insight into the effect of PrEE on transcriptional regulation in the cortex. The most significant interactions were found between PrEE and RZRβ, ephrin A5 and Id2 expression.

The dramatic upregulation of Id2, and correlated hypomethylation is a significant finding that may have far reaching effects and warrants a more thorough investigation. The importance of this discovery lies in the range of roles that Id2 plays. Included amongst these functions, Id2 plays a role in the regulation of cell proliferation, senescence, cell cycle control, apoptosis, angiogenesis and metastasis (Norton et al., 2000; Lasorella et al., 2001; Yokota and Mori, 2002; Uzinova and Benezra, 2003; Fong et al., 2004; Coma et al., 2010). More recently it has been proposed that Id2 is involved in cell priming, a process by which cells from varying tissues are sensitized, allowing a strong, complete response to biological or chemical signals (García-Trevijano et al., 2013). The effect of priming via Id2 is thought to be highly sensitive to the cell microenvironment, exacting its priming effect via the induction of an open chromatin structure (Norton et al., 2000; Lasorella et al., 2001; Fong et al., 2004; Coma et al., 2010; García-Trevijano et al., 2013). Furthermore, chromatin structure is directly influenced by DNA methylation, which working together, can regulate transcription (Kang et al., 2015). Work in this dissertation has demonstrated significant transgenerationally stable hypomethylation of Id2 DNA, suggesting the possibility of a novel Id2-mediated pathway by which PrEE could be impacting cortical development. A thorough investigation of downstream transcriptional events, translation and cofactor recruitment/association will be necessary to determine the undoubtedly complex role ethanol plays in Id2 function.

72

The neocortex of PrEE mice offspring had downregulated Ephrin A5 expression

in caudal cortex at P0. Although the nature of the relationship between PrEE and

Ephrin A5 expression in caudal cortex remains unknown, the degradation of

incoming activity to occipital/visual cortex may initiate abnormal cortical activity

leading to abnormal expression of Ephrin A5 at this age. Indeed, numerous

deficits in visual processing have been described in models of PrEE, including

retinal defects, microphthalmia and widespread apoptosis in the developing

visual system during synaptogenesis (Tenkova et al., 2003; Stenkamp et al.,

2009; Muralidharan et al., 2015). Global, and promoter-specific changes to

methylation described in the present work also open up the possibility that

hypermethylation of CpG islands in the promoter region of ephrin A5 are driving

the observed downregulation.

Hypomethylation of CpG islands in the promoter regions of Id2 and RZRβ, along

with global alterations to 5mc and 5hmc is correlated with increased transcription,

an effect that persists across generations. CpG island methylation in the

promoter region has been demonstrated to regulate transcription in distinct tissue

types (Choi et al., 2005; Meissner et al., 2008; Mohn et al., 2008; Moore et al.,

2013). We propose that PrEE is altering transcription across generations, in part,

by altering methylation patterns. We further propose that one mechanism by

which DNA methylation patterns are being altered is through the downregulation of DNA methyltransferases. These heritable changes are first generated with the initial ethanol insult during gestations where DNMT1, 3A and 3B function is perturbed. By impairing de novo methylation by DNMT3A and 3B we initiate a flawed DNA methylation program that is maintained by DNMT1, and passed along to successive, unexposed generations.

The work outlined in this dissertation provides insight into one effect of PrEE on the epigenome, and the transgenerational consequences of these changes. By further developing our understanding of the mechanisms by which PrEE alters the epigenome we will gain a more complete understanding of how ethanol impacts development, information which may help with the prevention and treatment of FASD.

Tables and Figures:

Table 1. List of abbreviations. Abbreviations listed for structures identified in figures and text.

Table 1	
Abbreviation	Structure
A1	Primary auditory cortex
BG	Basal ganglia
CA3	Cornu ammonis region 3, hippocampus
CC	Corpus callosum
dLGN	Dorsal lateral geniculate nucleus
DPL	Dye placement location
FAS	Fetal alcohol syndrome
FASD	Fetal alcohol spectrum disorders
FC	Frontal cortex
P	Postnatal day
PL	Prelimbic cortex
PrEE	Prenatal ethanol exposure
S1	Primary somatosensory cortex
V1	Primary visual cortex

Table 2. Cell packing density. Regional cortical cell packing densities measured in PrEE and control mice. 30μM coronal sections stained with cresyl violet were analyzed using the ICTN plugin for ImageJ. Data are presented as mean cells x 10^3/mm^3 ± s.e.m. No significant changes in cell packing density between experimental and control animals were detected.

Table 2

Cortical cell packing density in PrEE and control mice expressed in cells x 10^3/mm^3 as mean ± s.e.m.

	PL		dFC		S1		A1		V1	
	Con	PrEE	Con	PrEE	Con	PrEE	Con	PrEE	Con	PrEE
P0	101.4 ± 3.1	100.5 ± 1.9	102.6 ± 3.8	100.6 ± 2.7	115.5 ± 1.1	111.7 ± 1.4	104.7 ± 2.4	103.1 ± 2.0	121.0 ± 1.8	119.6 ± 2.3

Note: PL, prelimbic cortex; dFC, dorsal frontal cortex; S1, primary somatosensory cortex; A1, primary auditory cortex; V1, primary visual cortex.

Table 3. List of primer sequences. Primers for RT-qPCR were designed to span exon-exon boundaries to prevent amplification of gDNA. Primer efficiency was determined using a standard curve. Primers that did not fall between 95-100% efficiency were redesigned.

Table 3. RT-qPCR primer sequences

Target	Forward primer	Reverse primer
β Actin	CCATCATGAAGTGTGACGTGG	GTCCGCCTAGAAGCATTTGCG
Cad8	TGCACCTGAGTTCCTCAATGGAC	ATAATGGCTGTTTCAGGCTCAATG
EphA7	TTGGAAGAAGGCACTGTGGT	TAGGTTTTGGTGCCTGGAAA
Ephrin A5	CTACATCTCCTCTGCAATCCCA	GGCTGACTCATGTACGGTGT
Id2	ACATCAGCATCCTGTCCTTGCAG	AAGGTCCATTCAACGTGTTCTCC
LHX2	CTGCCGAGGGCTCACGAAG	AGAGAACCGCCTGTAGTAGTCT
RZR β	GGGCTGGGAGCTTCATGACTAC	GAAGAATCCCTTGCAGCCTTCAC

Table 4. Correlation of DNA methylation and RNA expression. Pearson correlations between DNA methylation and RNA expression were calculated for Id2 and RZRβ in cortical tissue. A strong, and significant, negative correlation between DNA methylation and RNA expression was identified in control and experimental groups for both id2 and RZRβ. Ten replicates were obtained for each condition. (*P < 0.05).

Table 4. Pearson correlations of methylation/expression

	Control	F1	F2	F3
Id2 M/E	-0.688*	-0.651*	-0.621*	-0.634*
RZRβ M/E	-0.692*	-0.634*	-0.711*	-0.664*

Note: *P<0.0.5, two-tailed, N=10. M/E, DNA promoter region methylation and RNA expression correlation.

Table 5. Correlations of behavioral performance. Pearson correlations were calculated between measures of anxiety, depression and sensorimotor integration. A moderate, significant, correlation was found between grooming and latency to leave center, two measures of anxiety. Grooming was also significantly correlated with both falls and missteps, two measures of sensorimotor integration. Falls were significantly correlated with missteps, depressive-like behavior (measured on FST) and motor learning/balance performance (measured on Accelerated Rotarod). Missteps were correlated with motor learning/balance performance. (*P < 0.05, **P < 0.01).

Table 5. Pearson correlations of behavioral performance

	Weight	LC	Groom	Falls	Missteps	FST
Weight						
LC	-0.071					
Groom	0.124	-0.382**				
Falls	0.070	0.113	-0.426**			
Missteps	-0.027	0.114	-0.351**	0.401**		
FST	0.103	0.233	-0.299	0.428**	0.226	
Rotarod	-0.074	-0.294	0.205	-0.503**	-0.360*	-0.280

Note: *P<0.05, **P<0.01, two-tailed, N=45. LC, latency to leave center; FST, Forced Swim Test.

Figure 1. Basic modifications of the epigenome. Epigenetic modifications regulate gene activity without modifying DNA sequence. The two most well studied modifications to the epigenome are DNA methylation and histone tail modifications. These modifications can be divided into two broad categories: activating and inactivating marks, distinctions that are made based on the modifications impact on transcription. DNA methylation of CpG islands in the promoter region of genes as well as certain histone modifications including trimethylation of H3K9 and H3K27 is typically associated with inactivation. These modifications cause chromatin to condense, packing nucleosomes tightly, limiting the accessibility of DNA to transcription factors, reducing expression. Histone tail modifications including monomethylation of H3K4 and H3K27, and acetylation of H3K9 and H3K14 promote slackening of chromatin increasing accessibility of DNA to transcription factors, increasing expression.
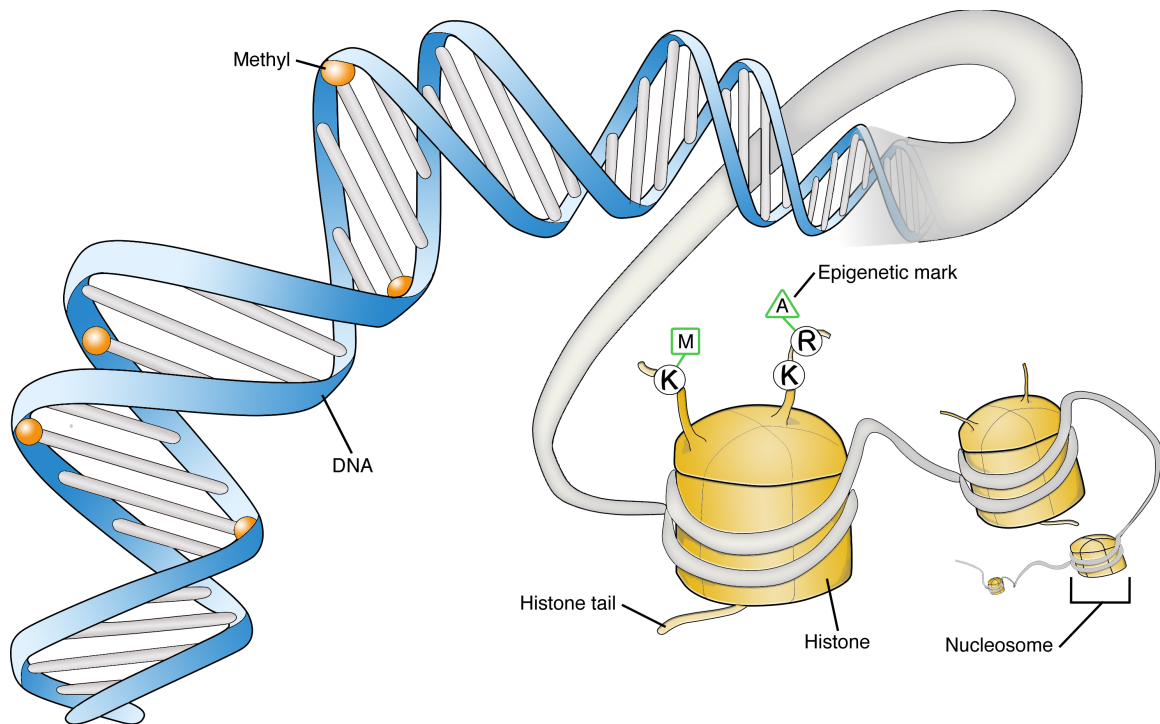
Figure 2. Measurements in ethanol (EtOH)-exposed and control dams. Black bars, EtOH-exposed dams; White bars, control dams. **A**, No significant differences were detected in average dam food intake. (EtOH-exposed, N = 24; control, N = 26). **B**, Average gestational weight gain (g). EtOH-exposed dams (N =12) gained significantly less weight during gestation when compared with controls (N =14; *P < 0.05). **C**, Average litter size. Gestational exposure to EtOH resulted in significantly reduced litter size in experimental cases (N =11) when compared with controls (N =10; *P = 0.05). **D**, No significant difference was detected in average dam liquid intake between control and experimental dams (EtOH-exposed, N = 24; control, N = 26). **E**, No significant difference was detected in average dam plasma osmolality (mosm/kg) between control and experimental dams (EtOH-exposed, N = 15; control, N = 15). **F**, Average dam blood ethanol content (mg/dl) at GD9 and GD19. EtOH-exposed dams (GD9 N = 11, GD19 N = 12) had elevated BEC levels compared to untreated controls (GD9 N = 5, GD19 N = 7; ***P < 0.001, ****P < 0.0001). On average, pregnant dams consumed 1.64 ml/day of 100% ethanol in a diluted solution.
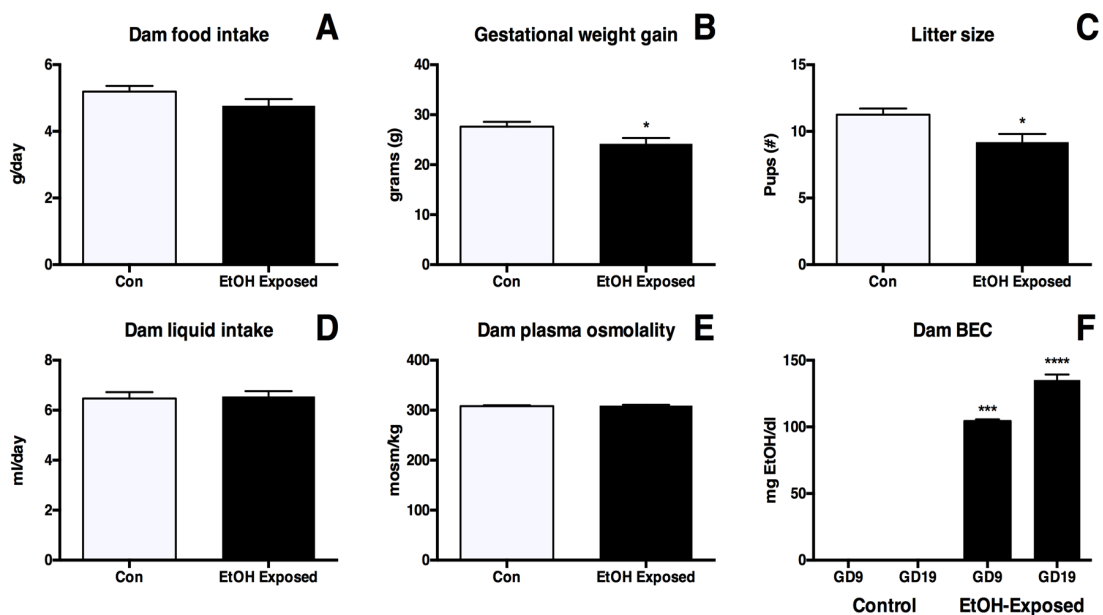
Figure 3. Anatomical volume and thickness measures in P0 PrEE and control mice. Panels are low magnification images of representative Nissl-stained 30μM coronal sections in control (top row) and PrEE mice (middle row). Outlines and arrows indicate area of measure. Significant reductions were detected across all regions investigated: dLGN (A3; n = 8, P < 0.05), basal ganglia (B3; n = 8, P < 0.01), CA3 pyramidal layer thickness (C3; n = 8, P < 0.01) and corpus callosum (D3; n = 8, P < 0.05). Data is expressed as mean percent of baseline corrected control ± S.E.M. Dorsal (D) up, lateral (L) to the right. Scale bars = 500 μM.
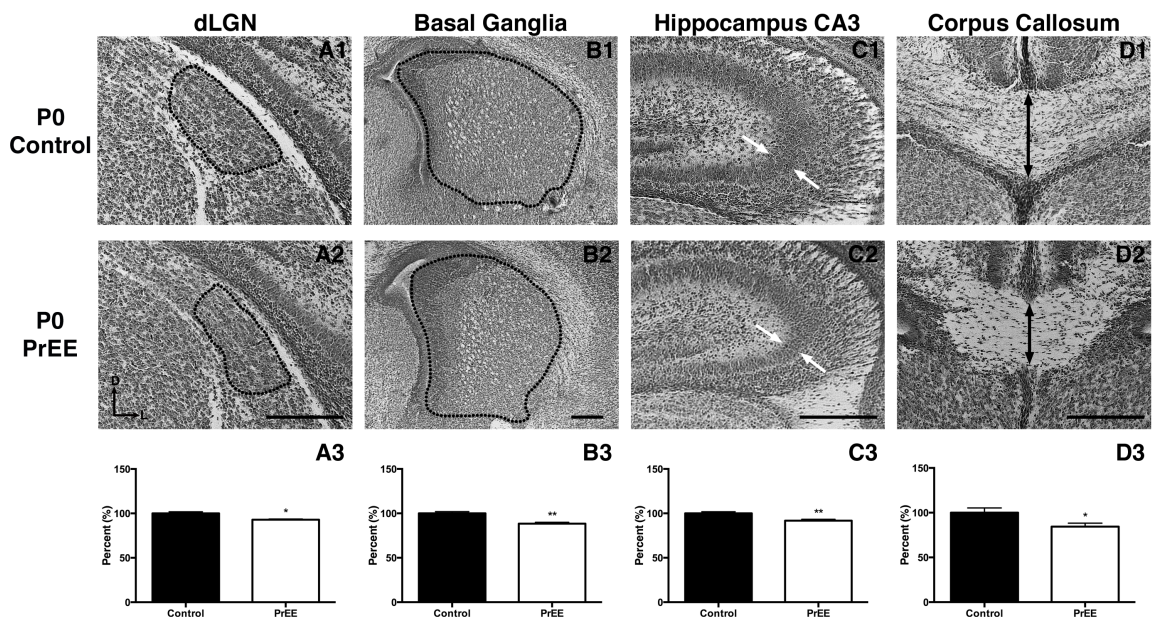
Figure 4. Cortical thickness measures in P0 PrEE and control mice.
Representative 30µM Nissl-stained coronal sections in control (top row) and
PrEE mice (middle row). Arrows indicate area of measure. A significant reduction
was detected in prelimbic (A3; n=15, P < 0.05) and auditory cortices (D3; n=15, P
< 0.0001). PrEE mice exhibited significantly thicker dorsal frontal (B3; n=15, P <
0.001), somatosensory (C3; n=15, P < 0.0001) and visual cortices (E3; n=15, P
< 0.0001). Data is expressed as mean percent of baseline corrected control ±
S.E.M. Dorsal (D) up, lateral (L) to the right. Scale bars = 500 µM.
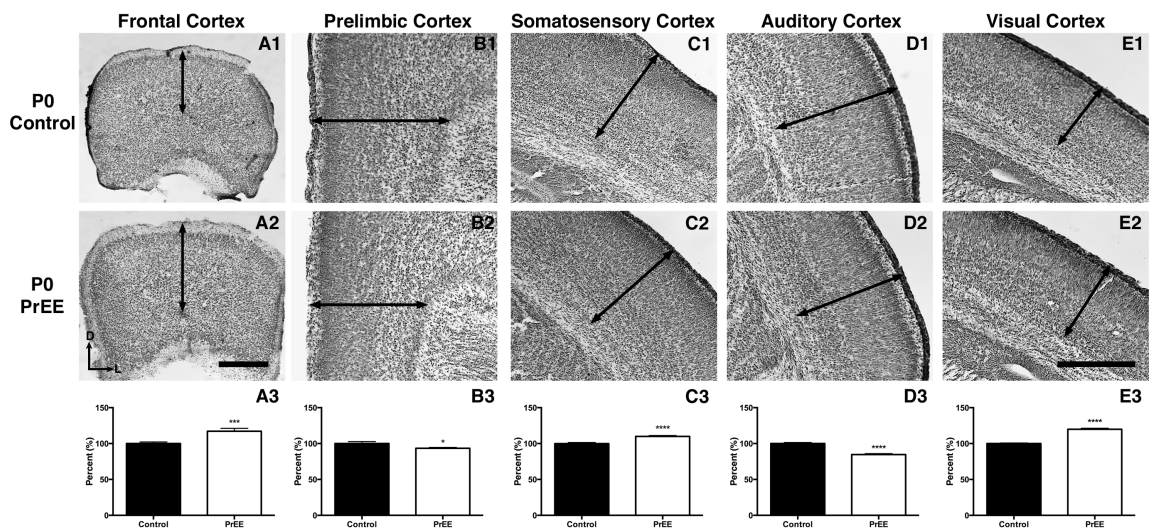
Figure 5. Neocortical expression of RZRβ, Cad8, and Id2. Coronal sections (100 µm) of P0 control and PrEE brain hemispheres following free-floating nonradioactive in situ hybridization with a probe against RZRβ (**A1**, **A2**, **B1**, **B2**), Cad8 (**C1**, **C2**) or Id2 (**D1**, **D2**). **A1**, Section through a caudal region of frontal cortex where left arrow denotes low medial cortical expression of RZRβ and a right arrow denotes moderate lateral expression in a control case. **A2**, Section through a caudal region of frontal cortex where left arrow denotes moderate medial cortical expression of RZRβ and a right arrow denotes high lateral expression in a PrEE case. **B1**, Section through a rostral region of parietal cortex where left black arrow denotes low medial cortical expression of RZRβ, a white middle arrow denotes the medial boundary of RZRβ expression, and a right arrow denotes moderate lateral expression of RZRβ in a control case. **B2**, Section through a rostral region of parietal cortex where left black arrow denotes moderate medial cortical expression of RZRβ, a white middle arrow denotes the shifted medial boundary of RZRβ expression and a right arrow denotes high lateral expression of RZRβ in a PrEE case. **C1**, Section through a rostral region of parietal cortex where black arrow denotes lateral boundary of Cad8 expression in a control case. **C2**, Section through a rostral region of parietal cortex where black arrow denotes a shifted lateral boundary of Cad8 expression in a PrEE case. **D1**, Section through a rostral region of parietal cortex where black arrow denotes an absence of Id2 expression within cortical layers 3 and 4 in a control case. **D2**, Section through a rostral region of parietal cortex where black arrow denotes an extension of the lateral Id2 expression within layers 3/4. **E1**, **E2**, Patterns of gene expression compressed onto a coronal reconstruction of control (**E1**) or PrEE (**E2**) brains. Patterned areas represent gene expression as follows: RZRβ, diagonal line area; Cad8, crossed line area; Id2, dotted area. Dark line, cortical outline. Sections oriented dorsal (D) up and lateral (L) right. A minimum of 5 replicates were obtained for each gene and condition.
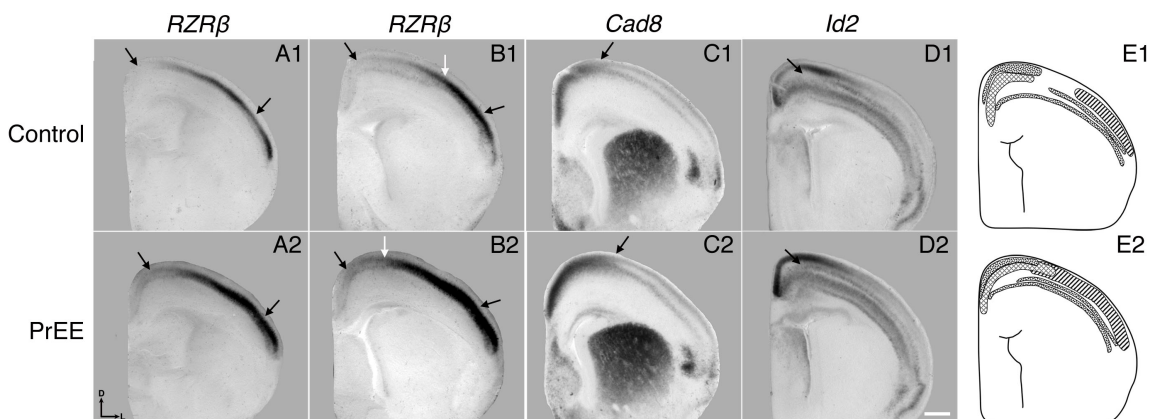
Figure 6. Analysis of neocortical expression of RZRβ, Cad8, and Id2. A1–D1.
Region of interest of quantified gene expression overlaid on representative
coronal brain illustrations corresponding to graphs below. **A2–D2**, Percentage
area fraction of cells expressing RZRβ (**A2**, **B2**), Cad8 (**C2**), Id2 (**D2**) within the
ROI of caudofrontal cortex (**A2**) and rostral parietal cortex (**B2–D2**). A sharply
increased percentage of transcripts are observed in PrEE cases when compared
with control animals. CC, corpus callosum; CP, caudoputamen; CTX, cortex; LSr,
lateral septal nucleus; Box, ROI. *P < 0.05, **P < 0.01, ***P < 0.001.
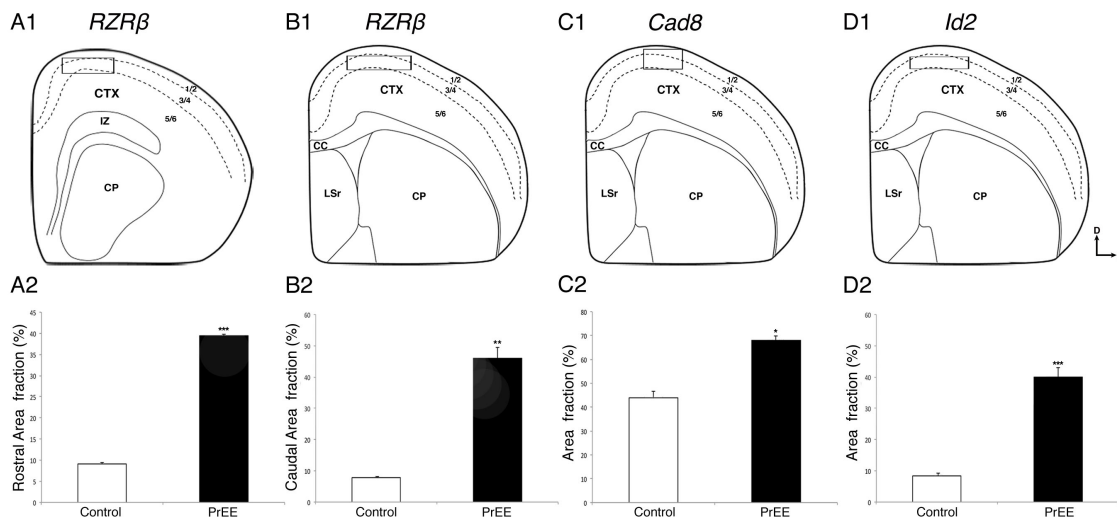
Figure 7. Average birth body weight, brain weight, and cortical length in PrEE and control P0 mice. **A**, Average pup body weight (g). PrEE F1 (n = 90), F2 (n = 38) and F3 pups (n = 25) had significantly lower birth weights compared with controls (n = 42). **B**, Average pup brain weight (g). PrEE F1 (n = 19), F2 (n = 20) and F3 pups (n = 20) had significantly lower brain weights at birth compared to controls (n = 23). **C**, Average pup cortical length (mm). PrEE F1 (n = 16), F2 (n = 15) and F3 pups (n = 10) had significantly lower cortical lengths compared with controls (n = 13). (*P < 0.05, **P < 0.01, ***P < 0.001, ****P < 0.0001).
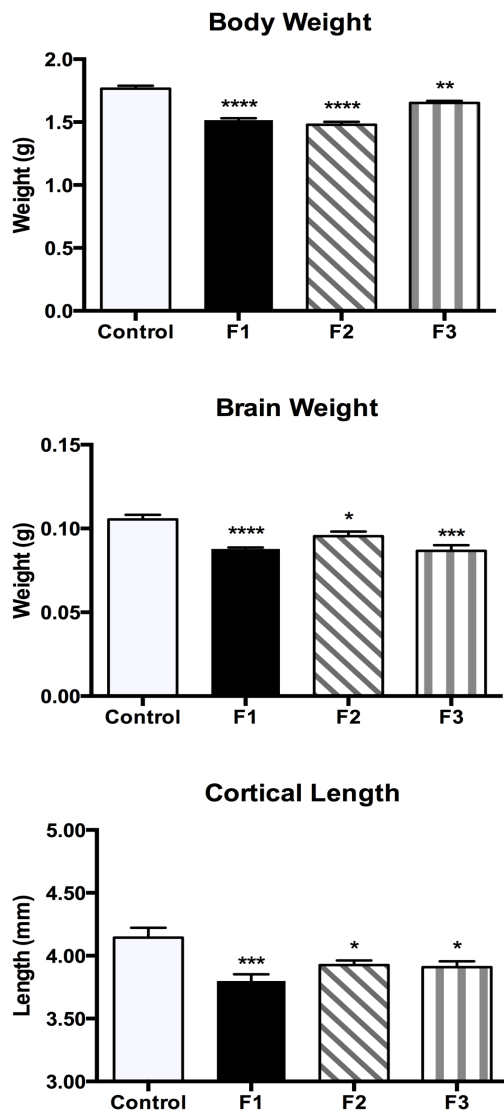
Figure 8. Analysis of rostral cortex INCs from visual cortex DPLs and caudal cortex INCs from somatosensory cortex DPLs. **A-A′**, Illustrations showing DPL (dot) and plane of section (dotted line). **B-E**, DAPI stained coronal sections (100 μm) of P0 hemispheres following DiI DPL in putative visual cortex in representative control (**B**) F1 (**C**), F2 (**D**) and F3 (**E**) cases. **B′-E′**, DAPI stained coronal sections (100 μm) of P0 hemispheres following DiI DPL in putative somatosensory cortex in representative control (**B′**) F1 (**C′**), F2 (**D′**) and F3 (**E′**) cases. **C-E′**, Arrows indicate ectopic retrogradely labeled cells. Dorsal (D) up and lateral (L) right. Scale bar, 500 μm. **F-F′** Labeled cell counts in rostral and caudal cortex. Rostral cortex (**F**) of F1, F2 and F3 PrEE animals had significantly more labeled cells resulting from a putative visual cortex DPL than controls. . Caudal cortex (**F′**) of F1, F2 and F3 PrEE animals had significantly more labeled cells resulting from a putative somatosensory cortex DPL when compared to controls. (*$P < 0.05$, **$P < 0.01$, ***$P < 0.001$).
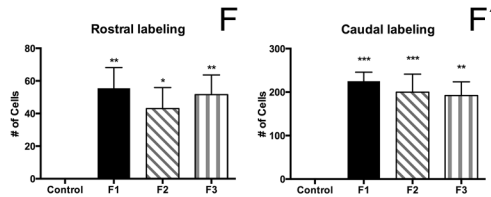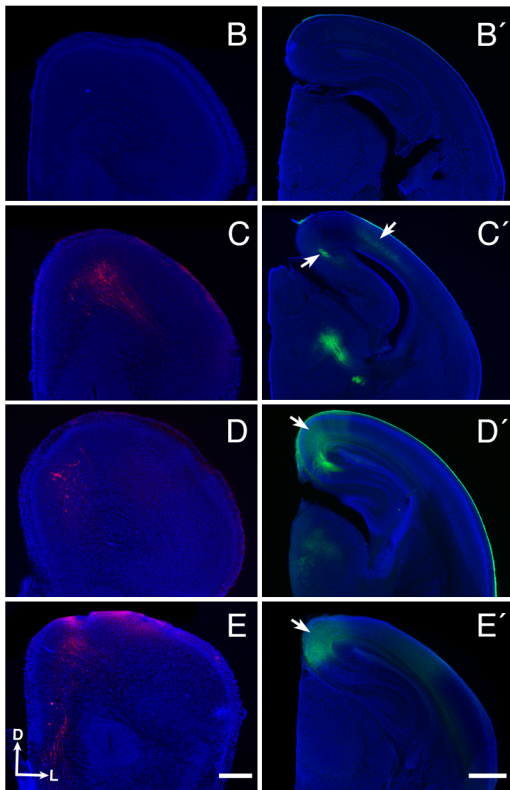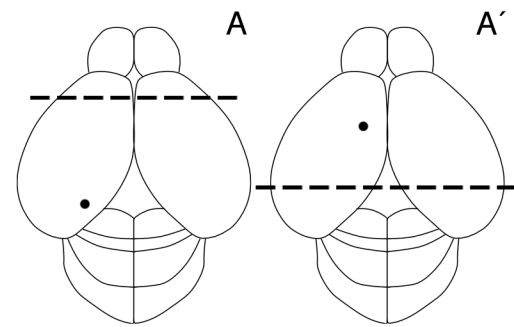
Figure 9. Log₂ normalized relative quantification of Ephrin A5, Eph A7, Cad8, Lhx2, Id2 and RZRβ expression across 3 generations using RT-qPCR. (**A**) Significant downregulation of Ephrin A5 expression was found in caudal cortex of F2 and F3 mice. (**B-D**) PrEE did not induce significant changes in Eph A7, Cad8 or Lhx2 expression when compared to controls. (**E**) Strong upregulation of Id2 was detected in rostral cortex of F2 and F3 mice, as well as caudal cortex of F1, F2 and F3 mice, when compared to controls. (**F**) Strong upregulation of RZRβ was detected in rostral cortex of F1, F2 and F3 mice, as well as caudal cortex of F2 and F3 mice, when compared to controls. Five biological replicates were obtained for each experimental condition. (***P < 0.001, ****P < 0.0001).
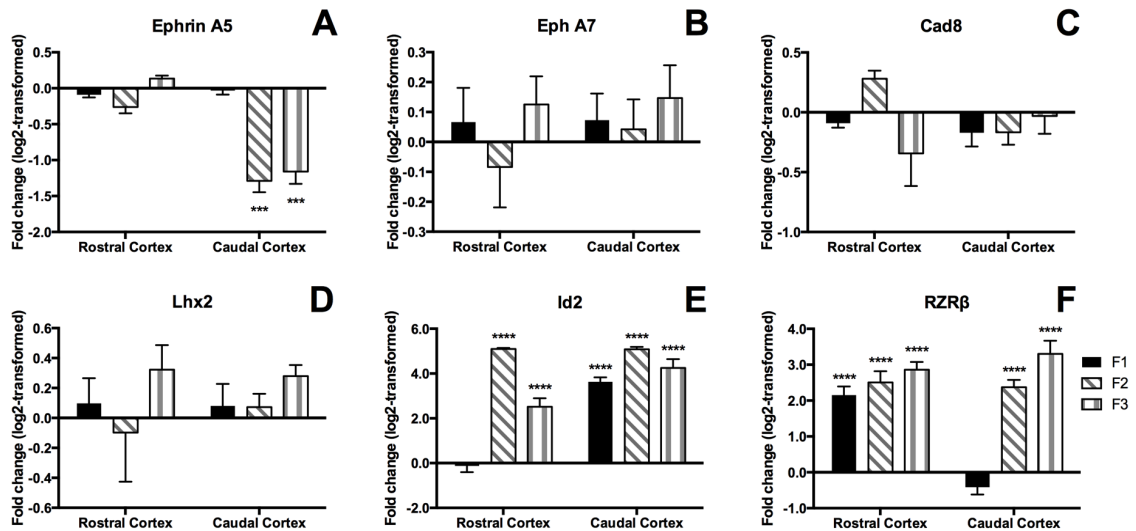
Figure 10. Log$_2$ normalized relative quantification of DNMT1, 3A and 3B expression across 3 generations. (**A-C**) RT-qPCR revealed significant downregulation of DNMT1 (A), DNMT3A (B) and DNMT3B in PrEE mice compared to controls. F2 and F3 mice descended from PrEE males showed no significant change from controls. Five biological replicates were obtained for each experimental condition. (****P < 0.0001).
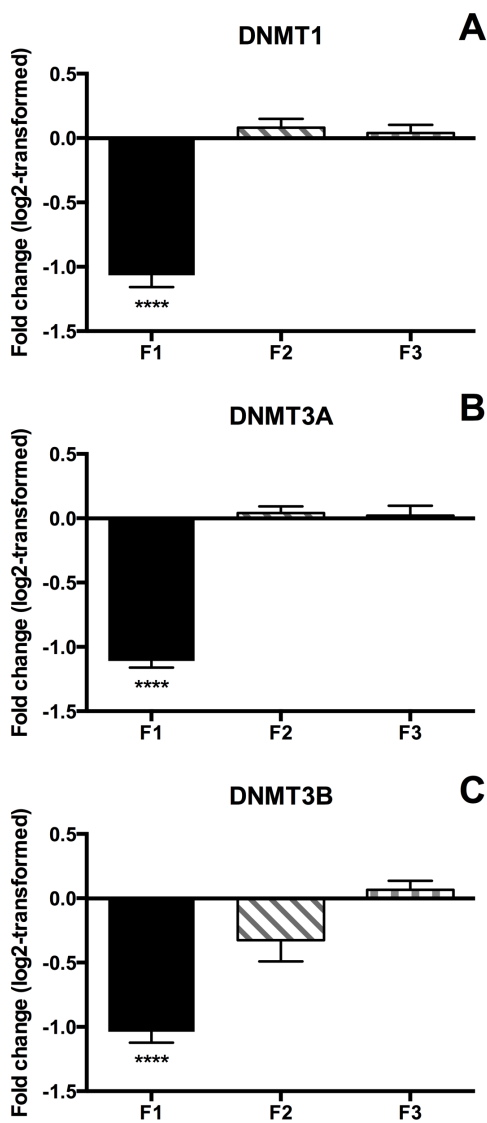
Figure 11. Global DNA methylation and hydroxymethylation in rostral and caudal cortical tissue. Colormetric assay was used to determine percent 5mc and 5hmc of total DNA in rostral and caudal regions of cortex. (**A**) Both rostral and caudal cortical global 5mC levels were significantly reduced in PrEE F1, F2 and F3 mice when compared to controls (n = 5 for each group). (**B**) Global 5hmc levels were significantly increased in rostral F1 cortex, when compared to controls. PrEE did not generate transgenerational changes to 5hmc levels. (n = 5 for each group). (**C**) Ratio of 5hmc to 5mc, is significantly increased in PrEE F1-F3 rostral cortex when compared to controls. In caudal regions of cortex F1 and F3 animals show a significant increase in 5hmc/5mc ratio. (*P < 0.05, **P < 0.01, ****P < 0.0001).
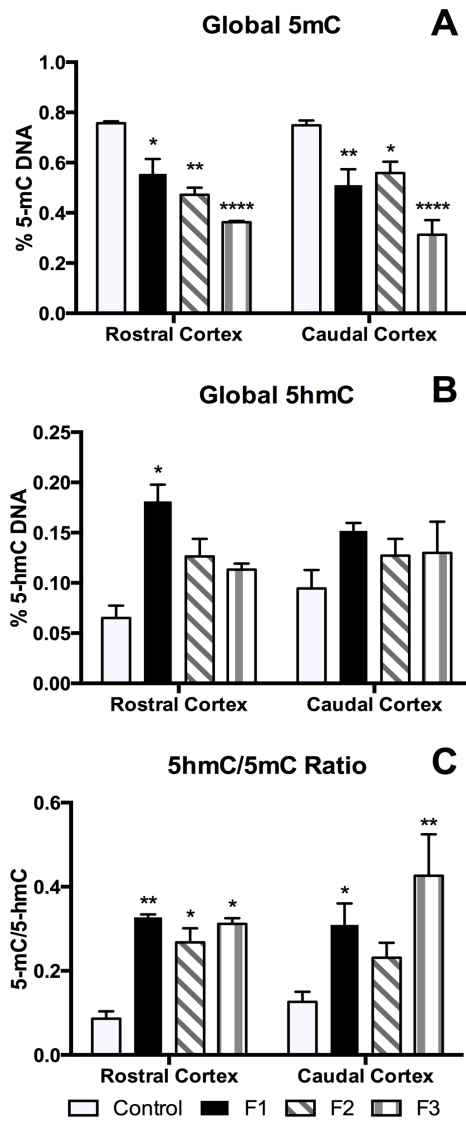
Figure 12. Methylation of CpG sites in the promoter region of Id2 and RZRβ.
Methylation specific PCR was used to determine promoter region methylation of two genes, Id2 and RZRβ, that were strongly upregulated. (**A**) CpG island methylation in the Id2 promoter region of both rostral and caudal cortical tissue from PrEE F1-F3 animals was significantly reduced when compared to controls. (**B**) CpG island methylation in the RZRβ promoter region of both rostral and caudal cortical tissue from PrEE F1-F3 animals was significantly reduced when compared to controls. Five biological replicates were obtained for each experimental condition. (***$P < 0.001$, ****$P < 0.0001$).
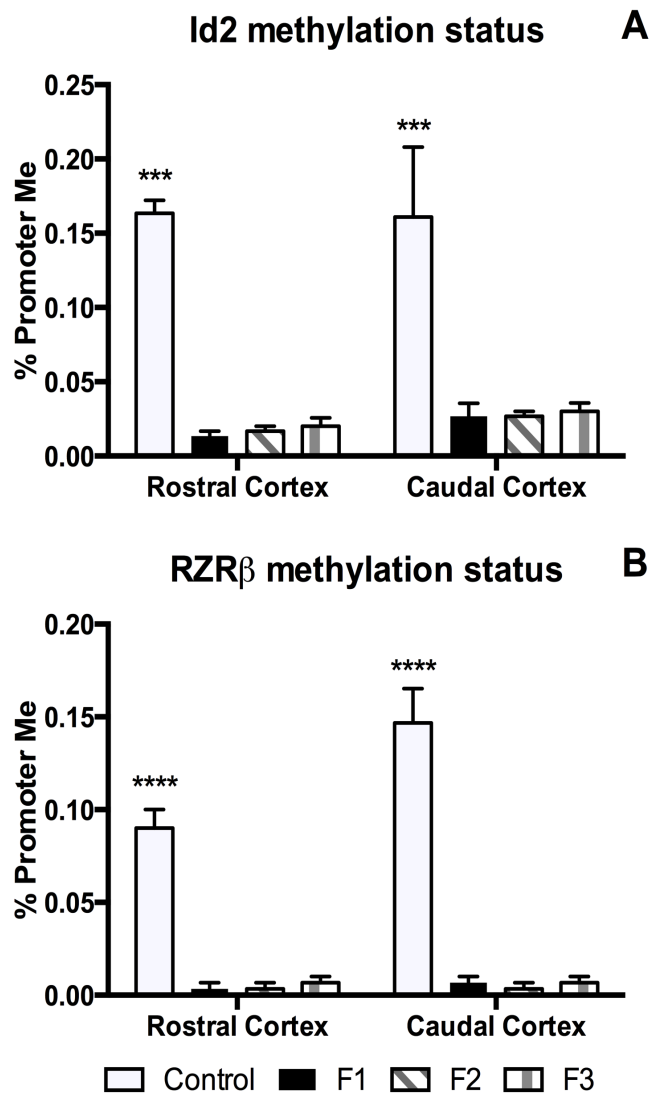
Figure 13. Behavioral measures in PrEE F1, F2 and F3 P30 mice. Motor function and learning, assayed using the Accelerated Rotarod (**A**), revealed significant reductions in F1 performance in trials 1 and 2. Significant group differences were found in measures of anxiety on the Suok apparatus: (**B**), Latency to leave center and (significant reductions in F1 and F2 animals) and (**C**), Stereotyped rearing/grooming (significant reductions in F1-F3 compared to controls). Significant group differences were also found in tests of motor coordination and sensorimotor integration: (**D**), Missteps and (**E**), Falls. In both measures, PrEE F1, F2 and F3 mice showed decreased motor coordination and sensorimotor integration compared with controls. Depressive-like behavior, measured as time spent immobile in the forced swim test (**F**), revealed significant increases in F1, F2 and F3 animals compared to controls. (*$P < 0.05$, **$P < 0.01$, ***$P < 0.001$, ****$P < 0.0001$).

A Rotarod

B Latency to leave center

C Rearing/Grooming

D Missteps

E Falls

F Forced Swim Test
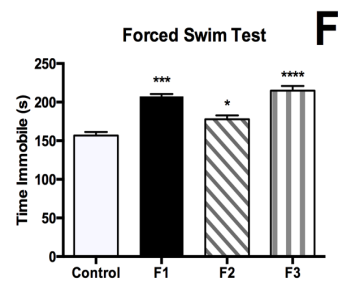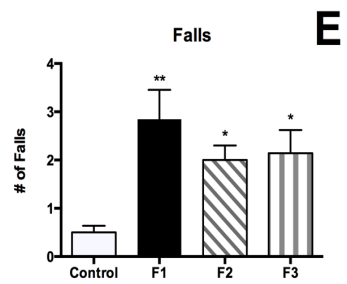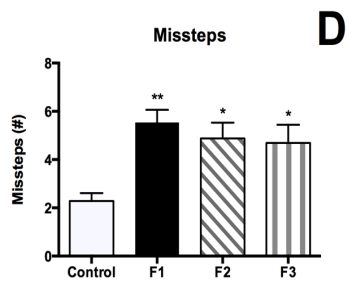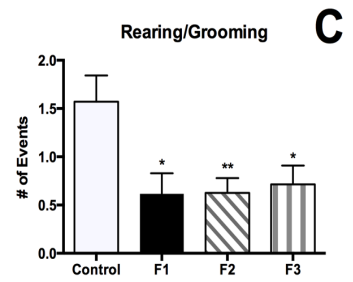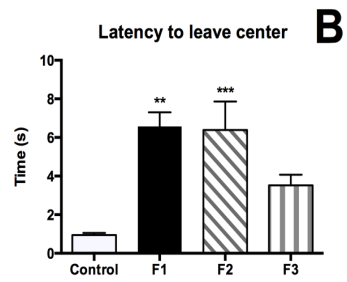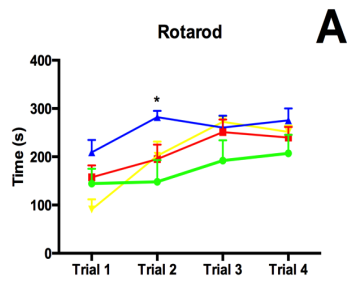
References

Abel EL, Sokol RJ. 1991. A revised conservative estimate of the incidence of FAS and its economic impact. Alcoholism: Clinical and Experimental Research. 15(3):514–524.

Abel EL. 1998. Fetal Alcohol Abuse Syndrome. New York; Plenum Press.

Adams J. 2008. Imprinting and genetic disease: Angelman, Prader-Willi and Beckwith-Weidemann syndromes. Nat. Educ. 1, 129.

Allan AM, Goggin SL, Caldwell KK. 2014. Prenatal alcohol exposure modifies glucocorticoid receptor subcellular distribution in the medial prefrontal cortex and impairs frontal cortex-dependent learning. PLoS One. 9(4):e96200.

Aoto K, Nishimura T, Eto K, Motoyama J. 2002. Mouse GLI3 regulates Fgf8 expression and apoptosis in the developing neural tube, face, and limb bud. Dev Biol. 251:320-332.

Archibald SL, Fennema-Notestine C, Gamst A, Riley EP, Mattson SN, Jernigan TL. 2001. Brain dysmorphology in individuals with severe prenatal alcohol exposure. Dev Med Child Neurol 43:148-54.

Armentano M, Chou SJ, Srubek Tomassy G, Leingartner A, O'Leary DD, Studer M. 2007. COUP-TFI regulates the balance of cortical patterning between frontal/motor and sensory areas. Nat Neurosci. 10:1277-1286.

Assimacopoulos S, Grove EA, Ragsdale CW. 2003. Identification of a Pax6-dependent epidermal growth factor family signaling source at the lateral edge of the embryonic cerebral cortex. J. Neurosci. 23:6399-6403.

Bachman M, Uribe-Lewis S, Yang X, Williams M, Murrell A, Balasubramanian S. 2014. 5-Hydroxymethylcytosine is a predominantly stable DNA modification. Nature chemistry. 6(12):1049–55.

Bartolomei MS. 2003. Epigenetics: role of germ cell imprinting. Adv Exp Med Biol. 518:239-245.

Bekdash RA, Zhang C, Sarkar DK. 2013. Gestational Choline Supplementation Normalized Fetal Alcohol-Induced Alterations in Histone Modifications, DNA Methylation, and Proopiomelanocortin (POMC) Gene Expression in β-Endorphin-

Producing POMC Neurons of the Hypothalamus. Alcohol Clin Exp Res. 37(7):1133-1142.

Bird AP, Taggart MH, Nicholls RD, Higgs DR. 1987. Non-methylated CpG-rich islands at the human alpha- globin locus: implications for evolution of the alpha-globin pseudogene. EMBO J. 6:999-1004.

Bishop KM, Goudreau G, O'Leary DD. 2000. Regulation of area identity in the mammalian neocortex by Emx2 and Pax6. Science. 288(5464):344–349.

Bishop KM, Rubenstein JL, O'Leary DD. 2002. Distinct actions of Emx1, Emx2, and Pax6 in regulating the specification of areas in the developing neocortex. J Neurosci. 22(17):7627-7638.

Blaess S, Stephen D, Joyner AL. 2008. Gli3 coordinates three-dimensional patterning and growth of the tectum and cerebellum by integrating Shh and Fgf8 signaling. Development. 135(12):2093-2103.

Bolz J, Uziel D, Muhlfriedel S, Gullmar A, Peuckert C, Zarbalis K, Wurst W, Torii M, Levitt, P. 2004. Multiple roles of ephrins during the formation of thalamocortical projections: maps and more. J Neurobiol. 59:82–94.

Bookstein FL, Connor PD, Huggins JE, Barr HM, Pimentel KD, Streissguth AP. 2007. Many infants prenatally exposed to high levels of alcohol show one particular anomaly of the corpus callosum. Alcohol Clin Exp Res 31:868-879.

Bookstein FL, Sampson PD, Connor PD, Streissguth AP. 2002. Midline corpus callosum is a neuroanatomical focus of fetal alcohol damage. Anat Rec Part B New Anat 269:162-174.

Borello U, Cobos I, Long JE, Murre C, Rubenstein JLR. 2008. FGF15 promotes neurogenesis and opposes FGF8 function during neocortical development. Neural Development. 3:17.

Borello U, Pierani A. 2010. Patterning the cerebral cortex: traveling with morphogens. Curr Opin Genet Dev. 20:408-415.

Bulchand S, Grove EA, Porter FD, Tole S. 2001. LIM-homeodomain gene Lhx2 regulates the formation of the cortical hem. Mech Dev. 100:165-175.

Burd L, Hofer R. 2008. Biomarkers for detection of prenatal alcohol exposure: a critical review of fatty acid ethyl esters in meconium. Birth Defects Research. Part A, Clinical And Molecular Teratology. 82(7):487-493.

Burd L, Klug MG, Martsolf JT, Kerbeshian J. 2003. Fetal alcohol syndrome: neuropsychiatric phenomics. Neurotoxicol Teratol. 25(6):697-705.

Bystron I, Blakemore C, Rakic P. Development of the human cerebral cortex: Boulder Committee revisited. Nature Reviews Neuroscience. 2008; 9(2):110-122.

Caetano R, Ramisetty-Mikler S, Floyd LR, et al. 2006. The epidemiology of drinking among women of childbearing age. Alcohol Clin Exp Res. 30:1023–1030.

Campi KL, Krubitzer L. 2010. Comparative studies of diurnal and nocturnal rodents: differences in lifestyle result in alterations in cortical field size and number. Journal of Comparative Neurology. 518:4491-4512.

Capel E, Fléjou JF, Hamelin R. 2007. Assessment of MLH1 promoter methylation in relation to gene expression requires specific analysis. Oncogene. 26:7596–7600.

Carmichael-Olsen H, Feldman JJ, Streissguth AP, Sampson PD, Bookstein FL. 1998. Neuropsychological deficits in adolescents with fetal alcohol syndrome: Clinical findings. Alcohol Clin Exp Res. 22:1998-2012.

Castellani V, Yue Y, Gao PP, Zhou R, Bolz J. 1998. Dual action of a ligand for Eph receptor tyrosine kinases on specific populations of axons during the development of cortical circuits. J Neurosci. 18:4663-4672.

Catania KC, Henry EC. 2006 Touching on somatosensory specializations in mammals. Current Opinion in Neurobiology. 16:467-473.

Catania KC. 2000. Cortical organization in Insectivora: The parallel evolution of the sensory periphery and the brain. Brain, Behavior and Evolution. 55:311–321.

Cavalli G. 2006. Chromatin and epigenetics in development: blending cellular memory with cell fate plasticity. Development. 133:2089-2094.

Center for Disease Control and Prevention (CDC). 1995. Update: Trends in fetal alcohol syndrome-United States, 1979-1993. Morbidity and Mortality Reports. 44(13):249-251.

Center for Disease Control and Prevention (CDC). 1997. Surveillance for fetal alcohol syndrome using multiple sources - Atlanta, Georgia, 1981-1989. Morbidity and Mortality Reports. 46(47):1118-1120.

Center for Disease Control and Prevention (CDC). 2002. Fetal alcohol syndrome—Alaska, Arizona, Colorado, and New York, 1995–1997. Morbidity and

Mortality Reports. 51(20):433-435.

Chabot N, Charbonneau V, Laramee ME, Tremblay R, Boire D, Bronchti G. 2008. Subcortical auditory input to the primary visual cortex in anophthalmic mice. Neurosci Lett. 433:129-134.

Chandramohan Y, Droste SK, Arthur JS, Reul JM. 2008. The forced swimming-induced behavioural immobility response involves histone H3 phosphoacetylation and c-Fos induction in dentate gyrus granule neurons via activation of the N-methyl-D- aspartate/extracellular signal-regulated kinase/mitogen- and stress-activated kinase signalling pathway. Eur J Neurosci. 27:2701-2713.

Chapin JK, Lin CS. 1984. Mapping the body representation in the SI cortex of anesthetized and awake rats. Journal of Comparative Neurology. 229:199-213.

Cheng LC, Tavazoie M, Doetsch F. 2005. Stem cells: from epigenetics to microRNAs. Neuron. 46:363-367.

Cheng X, Hsu CM, Currle DS, Hu JS, Barkovich AJ, Monuki ES. 2006. The roof plate has a central role in telencephalic development and holoprosencephaly. J Neurosci. 26(29):7640-7649.

Chenn A, Braisted J, McConnell S, O'Leary D.1997. Development of the cerebral cortex: mechanisms controlling cell fate, laminar and areal patterning, and axonal connectivity. In Molecular and Cellular Approaches to Neural Development, W.M. Cowan, L. Zipursky, and T. Jessell, eds. (Oxford: Oxford University Press), pp. 440–473.

Cholfin JA, Rubenstein JL. 2007. Patterning of frontal cortex subdivisions by Fgf17. Proceedings of the National Academy of Sciences U S A. 104(18):7652-7657.

Cholfin JA, Rubenstein JL. 2008. Frontal cortex subdivision patterning is coordinately regulated by Fgf8, Fgf17, and Emx2. J Comp Neurol. 509(2):144-155.

Chudley AE, Conry J, Cook JL, Loock C, Rosales T, LeBlanc N. 2005. Fetal alcohol spectrum disorder: Canadian guidelines for diagnosis. Can Med Assoc J. 172:S1–S21.

Church M, Kaltenbach J. 1997. Hearing, speech, language, and vestibular disorders in the fetal alcohol syndrome: A literature review. Alcohol Clin Exp Res 21:495-512.

Church MW, Hotra JW, Holmes PA, Anumba JI, Jackson DA, Adams BR. 2012. Auditory brainstem response (ABR) abnormalities across the life span of rats prenatally exposed to alcohol. Alcohol Clin Exp Res 36:83-96.

Clarren SK, Smith DW. 1978. The fetal alcohol syndrome. Lamp. 35(10):4-7. Coma S, Amin DN, Shimizu A, Lasorella A, Lavarone A, Klagsbrun M. 2010. Id2 promotes tumor cell migration and invasion through transcriptional repression of semaphorin 3F. Cancer Res. 70(9), 3823-32.

Connor PD, Mahurin R. 2001. A preliminary study of working memory in fetal alcohol damage using fMRI. JINS. 7(2):206-214.

Connor PD, Sampson PD, Streissguth AP, Bookstein FL, Barr HM. 2006. Effects of prenatal alcohol exposure on fine motor coordination and balance: A study of two adult samples. Neuropsychologia. 44(5):744-751.

Crossley PH, Martin GR. 1995. The mouse Fgf8 gene encodes a family of polypeptides and is expressed in regions that direct outgrowth and patterning in the developing embryo. Development. 121:439-451.

Crossley PH, Martinez S, Ohkubo Y, Rubenstein JL. 2001. Coordinate expression of Fgf8, Otx2, Bmp4, and Shh in the rostral prosencephalon during development of the telencephalic and optic vesicles. Neuroscience. 108:183-206.

Cullen CL, Burne THJ, Lavidis NA, Moritz KM. 2014. Low dose prenatal alcohol exposure does not impair spatial learning and memory in two tests in adult and aged rats. PLoS ONE 9:e101482

Datta S, Turner D, Singh R, Ruest LB, Pierce WM, Jr, Knudsen TB. 2008. Fetal alcohol syndrome (FAS) in C57BL/ 6 mice detected through proteomics screening of the amniotic fluid. Birth Defects Research Part A, Clinical and Molecular Teratology. 82(4):177-186.

Davison JM, Mellott TJ, Kovacheva VP, Blusztajn JK. 2009. Gestational choline supply regulates methylation of histone H3, expression of histone methyltransferases G9a (Kmt1c) and Suv39h1 (Kmt1a), and DNA methylation of their genes in rat fetal liver and brain. J Biol Chem. 284(4), 1982-1989.

De Giorgio A, Granato A. 2015. Reduced density of dendritic spines in pyramidal neurons of rats exposed to alcohol during early postnatal life. Int J Dev Neurosci. 41:74-9.

Dehay C, Horsburgh G, Berland M, Killackey H, Kennedy H .1991. The effects of

bilateral enucleation in the primate fetus on the parcellation of visual cortex. Brain Res Dev Brain Res. 62:137-141.

Dehay C, Kennedy H. 2007. Cell-cycle control and cortical development. Nat Rev Neurosci. 8:438-450.

Deng G, Chen A, Pong E, Kim YS. 2001. Methylation in hMLH1 promoter interferes with its binding to transcription factor CBF and inhibits gene expression. Oncogene. 20:7120–7127.

Derauf C, Kekatpure M, Neyzi N, Lester B, Kosofsky B. 2009. Neuroimaging of children following prenatal drug exposure. Semin Cell Dev Biol 20:441-454.

Devinsky O, D'Esposito M. 2004. Neurology of Cognitive and Behavioral Disorders. Oxford University Press, New York.

Dokmanovic M, Marks PA. 2005. Prospects: histone deacetylase inhibitors. J Cell Biochem. 96:293-304.

Dufour A, Seibt J, Passante L, Depaepe V, Ciossek T, Frisen J, Kullander K, Flanagan JG, Polleux F, Vanderhaeghen P. 2003. Area specificity and topography of thalamocortical projections are controlled by ephrin/Eph genes. Neuron. 39:453-465.

Dunty WCJ, Chen S, Zucker RM, Dehart DB, Sulik KK. 2001. Selective vulnerability of embryonic cell populations to ethanol-induced apoptosis: implications for alcohol-related birth defects and neurodevelopmental disorder. Alcohol Clin Exp Res 25:1523–1535.

Dye CA, Abbott CW, Huffman KJ. 2012. Bilateral enucleation alters gene expression and intraneocortical connections in the mouse. Neural Dev. 30:7:5.

Dye CA, El Shawa H, Huffman KJ. 2011a. A Lifespan Analysis of Intraneocortical Connections and Gene Expression in the Mouse I. Cereb Cortex. 21:1311-1330.

Dye CA, El Shawa H, Huffman KJ. 2011b. A Lifespan Analysis of Intraneocortical Connections and Gene Expression in the Mouse I. Cereb Cortex. 21:1331-1350.

Egea J, Klein R. 2007. Bidirectional Eph-ephrin signaling during axon guidance. Trends Cell Biol. 17:230–238.

El Shawa H, Abbott CW, Huffman KJ. 2013. Prenatal ethanol exposure disrupts intraneocortical circuitry, cortical gene expression, and behavior in a mouse model of FASD. J Neurosci. 33(48):18893-18905.

Ethen MK, Ramadhani TA, Scheuerle AE, Canfield MA, Wyszynski DF, Druschel CM, Romitti PA. 2009. Alcohol consumption by women before and during pregnancy. Matern Child Health J. 12:274-285.

Faedo A, Tomassy GS, Ruan Y, Teichmann H, Krauss S, Pleasure SJ, Tsai SY, Tsai MJ, Studer M, Rubenstein JL. 2008. COUP-TFI coordinates cortical patterning, neurogenesis, and laminar fate and modulates MAPK/ERK, AKT, and beta-catenin signaling. Cereb Cortex. 18:2117-2131.

Falls JG, Pulford DJ, Wylie AA, Jirtle RL. 1999. Genomic imprinting: implications for human disease. Am J Pathol. 154:635–647

Fernandes M, Gutin G, Alcorn H, McConnell SK, Hébert JM. 2007. Mutations in the BMP pathway in mice support the existence of two molecular classes of holoprosencephaly. Development. 134(21):3789-3794.

Fernández-Jaén A, Fernández-Mayoralas DM, Quiñones Tapia D, Calleja-Pérez B, García-Segura JM, Arribas SL, Muñoz Jareño N. 2011. Cortical thickness in fetal alcohol syndrome and attention deficit disorder. Pediatr Neurol 45:387-391.

Ficz G, Branco MR, Seisenberger S, Santos F, Krueger F, Hore TA, et al. 2011. Dynamic regulation of 5-hydroxymethylcytosine in mouse ES cells and during differentiation. Nature. 473:398–402.
Finer LB, Henshaw SK. 2006. Disparities in rates of unintended pregnancy in the United States, 1994 and 2001. Perspect Sex Reprod Health. 38:90-96.

Floyd RL, Sidhu JS. 2004. Monitoring prenatal alcohol exposure. Am J Med Genet C Semin Med Genet. 127:3-9.

Fong S, Debs RJ, Desprez PY. 2004. Id genes and proteins as promising targets in cancer therapy. Trends Mol Med. 10(8), 387-92.

Fukuchi-Shimogori T, Grove EA. 2001. Neocortex patterning by the secreted signaling molecule FGF8. Science. 294(5544):1071-1074.

Fukuchi-Shimogori T, Grove EA. 2003. Emx2 patterns the neocortex by regulating FGF positional signaling. Nat Neurosci. 6(8):825-831.

Galceran J, Miyashita-Lin EM, Devaney E, Rubenstein JL, Grosschedl R. 2000.

Hippocampus development and generation of dentate gyrus granule cells is regulated by LEF1. Development. 127(3):469-482.

Garcia-Algar O, Kulaga V, Gareri J, Koren G, Vall O, Zuccaro P, et al. 2008. Alarming prevalence of fetal alcohol exposure in a Mediterranean city. Therapeutic Drug Monitoring. 30(2):249-254.

García-Trevijano ER, Torres L, Zaragozá R, Viña JR. 2013. The Role of Id2 in the Regulation of Chromatin Structure and Gene Expression, Chromatin Remodelling, Dr. Danuta Radzioch (Ed.), ISBN: 978-953-51-1087-3, InTech, DOI: 10.5772/54969.

Gardiner-Garden M, Frommer M. 1987. CpG islands in vertebrate genomes. J Mol Biol. 196:261-282.

Garel S, Huffman KJ, Rubenstein JLR. 2003. A caudal shift in neocortical patterning in a Fgf8 hypomorphic mouse mutant. Development. 130:1903-1914.

Garel S, Rubenstein JLR. 2004. The Cognitive Neurosciences, M. S. Gazzaniga, Ed. (MIT Press, Cambridge, MA, 3rd ed.), pp. 69–84.

Gareri J, Lynn H, Handley M, Rao C, Koren G. 2008. Prevalence of fetal ethanol exposure in a regional population- based sample by meconium analysis of fatty acid ethyl esters. Therapeutic Drug Monitoring. 30(2):239-45.

Gautam P, Nuñez SC, Narr KL, Kan EC, Sowell ER. 2014. Effects of prenatal alcohol exposure on the development of white matter volume and change in executive function. Neuroimage Clin 4;5:19-27.

Gitton Y, Cohen-Tannoudji M, Wassef M. 1999. Role of thalamic axons in the expression of H-2Z1, a mouse somatosensory cortex specific marker. Cereb Cortex. 9:611-620.

Godin EA, Dehart DB, Parnell SE, O'Leary-Moore SK, Sulik KK. 2011. Ventromedian forebrain dysgenesis follows early prenatal ethanol exposure in mice. Neurotoxicol Teratol 33:231-9.

Govorko D, Bekdash RA, Zhang C, Sarkar DK. 2012. Male germline transmits fetal alcohol adverse effect on hypothalamic proopiomelanocortin gene across generations. Biol Psychiatry. 72:378–388.

Green ML, Singh AV, Zhang Y, Nemeth KA, Sulik KK, Knudsen TB. 2007. Reprogramming of genetic networks during initiation of the Fetal Alcohol

Syndrome. Dev Dyn. 236:613-631.

Grove EA, Fukuchi-Shimogori T. 2003. Generating the cerebral cortical area map. Annual Review of Neuroscience. 26:355-380.

Grove EA, Tole S, Limon J, Yip L, Ragsdale CW. 1998. The hem of the embryonic cerebral cortex is defined by the expression of multiple Wnt genes and is compromised in Gli3-deficient mice. Development. 125:2315–2325.

Hajkova P, Erhardt S, Lane N, Haaf T, El-Maarri O, Reik W, Walter J, Surani MA. 2002. Epigenetic reprogramming in mouse primordial germ cells. Mech Dev. 117(1-2):15-23.

Hansen DV, Lui JH, P. R, Kriegstein AR. 2010. Neurogenic radial glia in the outer subventricular zone of human neocortex. Nature. 464(7288):554-561.

Haycock PC, Ramsay M. 2009. Exposure of Mouse Embryos to Ethanol During Preimplantation Development: Effect on DNA Methylation in the H19 Imprinting Control Region. Biol Reprod. 81(4):618-27.

Health Canada. 2011. The Canadian Alcohol and Drug Use Monitoring Survey (CADUMS).

Hebert JM, Lin M, Partanen J, Rossant J, McConnell SK. 2003. FGF signaling through FGFR1 is required for olfactory bulb morphogenesis. Development. 130(6):1101-1111.

Hebert JM, McConnell SK. 2000. Targeting of cre to the Foxg1 (BF-1) locus mediates loxP recombination in the telencephalon and other developing head structures. Developmental Biology. 222(2):296-306.

Hellemans KG, Sliwowska JH, Verma P, Weinberg J. 2010. Prenatal alcohol exposure: fetal programming and later life vulnerability to stress, depression and anxiety disorders. Neurosci Biobehav Rev. 34:791– 807.

Hellemans KG, Verma P, Yoon E, Yu WK, Young AH, Weinberg J. 2010. Prenatal alcohol exposure and chronic mild stress differentially alter depressive- and anxiety-like behaviors in male and female offspring. Alcohol Clin Exp Res. 34:633-645.

Hikosaka O, Nakamura K, Sakai K, Nakahara H. 2002. Central mechanisms of motor skill learning. Curr Opin Neurobiol. 12:217-222.

Hoch RV, Rubenstein JL, Pleasure S. 2009. Genes and signaling events that establish regional patterning of the mammalian forebrain. Seminars in Cell and Developmental Biology. 20(4):378-386.

Holmes A, Fitzgerald PJ, MacPherson KP, DeBrouse L, Colacicco G, Flynn SM, et al. 2012. Chronic alcohol remodels prefrontal neurons and disrupts NMDAR-mediated fear extinction encoding. Nat Neurosci. 15:1359–61.

Hoyme HE, May PA, Kalberg WO, Kodituwakku P, Gossage JP, Trujillo PM, Buckley DG, Miller JH, Aragon AS, Khaole N, Viljoen DL, Jones KL, et al. 2005. A practical clinical approach to diagnosis of fetal alcohol spectrum disorders: clarification of the 1996 institute of medicine criteria. Pediatrics. 115:39–47.

Huffman KJ, Garel S, and Rubenstein JLR. 2004. Fgf8 regulates the development of intra-neocortical projections. J Neurosci. 24:8917-8923.

Hutson J, Magri R, Gareri J, Koren G. 2010. The incidence of prenatal alcohol exposure in Montevideo Uruguay as determined by meconium analysis. Therapeutic Drug Monitoring. 32(3):311-317.

Institute of Medicine, and National Academy of Sciences USA. 1998. Choline. In: Dietary reference intakes for folate, thiamin, riboflavin, niacin, vitamin B12, pantothenic acid, biotin, and choline Vol. 1. National Academy Press, Washington DC, pp. 390– 422.

Ishii T, Hashimoto E, Ukai W, Tateno M, Yoshinaga T, Ono T, Watanabe K, Saito S, Saito T. 2008. Epigenetic regulation in alcohol-related brain damage. Nihon Arukoru Yakubutsu Igak-kai Zasshi. 43:705–713

Izraeli R, Koay G, Lamish M, Heicklen-Klein AJ, Heffner HE, Heffner RS, Wollberg Z. 2002. Cross-modal neuroplasticity in neonatally enucleated hamsters: structure, electrophysiology and behaviour. Eur J Neurosci. 15:693-712.

Jabaudon D, Shnider S, Tischfield D, Galazo M, Macklis JD. 2012. RORB overexpression induces barrel-like neuronal clusters in the developing neocortex. Cereb. Cortex. 22, 996-1006.

Jacobson JL, Jacobson SW, Sokol RJ. 1996. Increased vulnerability to alcohol-related birth defects in the offspring of mothers over 30. Alcohol Clin Exp Res. 20:359-363.

Jensen HH, Batres-Marquez SP, Carriquiry A, Schalinske KL. 2007. Choline in

the diets of the U.S. population: NHANES, 2003–2004. FASEB J 21:lb219.

Jenuwein T, Allis CD. 2001. Translating the histone code. Science. 293:1074-1080.

Jirikowic TL, McCoy SW, Lubetzky-Vilnai A, Price R, Ciol MA, Kartin D, Hsu LY, Gendler B, Astley SJ. 2013. Sensory control of balance: a comparison of children with fetal alcohol spectrum disorders to children with typical development. J Popul Ther Clin Pharmacol 20:e212-28.

Jones KL, Smith DW, Ulleland CN, Streissguth AP. 1973. Pattern of malformation in offspring of chronic alcoholic mothers. Lancet 1:1267– 1271.

Jones KL, Smith DW. 1973. Recognition of the fetal alcohol syndrome in early infancy. Lancet. 302: 999–1001.

Jones PA: The DNA methylation paradox. Trends Genet 1999, 15:34-37.

Kafri T, Ariel M, Brandeis M, Shemer R, Urven L, McCarrey J, Cedar H, Razin A. 1992. Developmental pattern of gene-specific DNA methylation in the mouse embryo and germ line. Genes Dev. 6:705-714.

Kahn DM, Krubitzer L. 2002a. Massive cross-modal cortical plasticity and the emergence of a new cortical area in developmentally blind mammals. Proc Natl Acad Sci USA. 99:11429-11434.

Kalueff AV, Keisala T, Minasyan A, Kumar SR, LaPorte JL, Murphy DL, Tuohimaa P. 2008. The regular and light-dark Suok tests of anxiety and sensorimotor integration: utility for behavioral characterization in laboratory rodents. Nat Protoc 3:129-136.

Kaneko WM, Ehlers CL, Philips EL, Riley EP. 1996a. Auditory event-related potentials in fetal alcohol syndrome and Down's syndrome children. Alcohol Clin Exp Res. 20(1):35-42.

Kaneko WM, Phillips EL, Riley EP, Ehlers CL. 1996b. EEG findings in fetal alcohol syndrome and Down syndrome children. Electroencephalogr Clin Neurophysiol. 98(1):20-28.

Kang JY, Song SH, Yun J, Jeon MS, Kim HP, Han SW, Kim TY. 2015. Disruption of CTCF/cohesin-mediated high-order chromatin structures by DNA methylation downregulates PTGS2 expression. Oncogene.

Karlen SJ, Krubitzer L. 2009. Effects of bilateral enucleation on the size of visual and nonvisual areas of the brain. Cereb Cortex. 19:1360-1371.

Kass SU, Landsberger N, Wolffe AP. 1997. DNA methylation directs a time-dependent repression of transcription initiation. Curr Biol. 7:157-165.

Kiefer JC. 2007. Epigenetics in development. Dev Dyn. 236:1144-1156.

Kleiber ML, Diehl EJ, Laufer BI, Mantha K, Chokroborty-Hoque A, Alberry B, Singh SM. 2014. Long-term genomic and epigenomic dysregulation as a consequence of prenatal alcohol exposure: a model for fetal alcohol spectrum disorders. Front Genet 5:161.

Klose RJ, Bird AP. 2006. Genomic DNA methylation: the mark and its mediators. Trends Biochem Sci. 31(2):89–97.

Kornberg RD, Lorch Y. 1999. Twenty-five years of the nucleosome, fundamental particle of the eukaryote chromosome. Cell. 98:285-294.

Kovacheva VP, Mellott TJ, Davison JM, Wagner N, Lopez-Coviella I, Schnitzler AC, Blusztajn JK. 2007. Gestational choline deficiency causes global and Igf2 gene DNA hypermethylation by up-regulation of Dnmt1 expression. J Biol Chem. 282:31777–31788.

Kriegstein AR, Noctor SC. 2004. Patterns of neuronal migration in the embryonic cortex. Trends Neurosci. 27:392–399.

Kulaga V, Shor S, Koren G. 2010. Correlation between drugs of abuse and alcohol by hair analysis: parents at risk for having children with fetal alcohol spectrum disorder. Alcohol. 44(7-8):615-621.

Kuschel S, Ruther U, Theil, T. 2003. A disrupted balance between Bmp/Wnt and Fgf signaling underlies the ventralization of the Gli3 mutant telencephalon. Dev Biol. 260:484-495.

Kvigne VL, Leonardson GR, Borzelleca J, Welty TK. 2008. Characteristics of grandmothers who have grandchildren with fetal alcohol syndrome or incomplete fetal alcohol syndrome. Matern Child Health J 12:760–765.

Lantz CL, Pulimood NS, Rodrigues-Junior WS, Chen CK, Manhaes AC, Kalatsky VA, Medina AE. 2014. Visual defects in a mouse model of fetal alcohol spectrum disorder. Front Pediatr. 9;2:107.

Lantz CL, Sipe GO, Wong EL, Majewska AK, Medina AE. 2015. Effects of Developmental alcohol exposure on potentiation and depression of visual cortex responses. Alcohol Clin Exp Res. 39(8):1434-42.

Larsen F, Gundersen G, Lopez R, Prydz H. 1992. CpG islands as gene markers in the human genome. Genomics. 13:1095-1107.

Lasorella A, Uo T, Lavarone A. 2001. Id proteins at the cross-road of development and cancer. Oncogene. 20, 8326-8333.

Laufer BI, Mantha K, Kleiber ML, Diehl EJ, Addison SM, Singh SM. 2013. Long-lasting alterations to DNA methylation and ncRNAs could underlie the effects of fetal alcohol exposure in mice. Dis Model Mech. 6(4):977-92.

Lebel C, Rasmussen C, Wyper K, Walker L, Andrew G, Yager J, Beaulieu C. 2008. Brain diffusion abnormalities in children with fetal alcohol spectrum disorder. Alcohol Clin Exp Res 32:1732-1740.

Lebel C, Roussotte F, Sowell ER. 2011. Imaging the impact of prenatal alcohol exposure on the structure of the developing human brain. Neuropsyhcol Rev 21:102-118.

Lee SM, Tole S, Grove E, McMahon AP. 2000. A local Wnt-3a signal is required for development of the mammalian hippocampus. Development. 127(3):457-467.

Leigland LA, Ford MM, Lerch JP, Kroenke CD. 2013. The influence of fetal ethanol exposure on subsequent development of the cerebral cortex as revealed by magnetic resonance imaging. Alcohol Clin Exp Res 37(6):924-32.

Li Z, Ma X, Peltier S, Hu X, Coles CD, Lynch ME. 2008. Occipital- temporal reduction and sustained visual attention deficit in prenatal alcohol exposed adults. Brain Imaging Behav 2:39-48.

Liu Y, Balaraman Y, Wang G, Nephew KP, Zhou FC. 2009. Alcohol exposure alters DNA methylation profiles in mouse embryos at early neurulation. Epigenetics. 4:500-511.

Livy DJ, Elberger AJ. 2008. Alcohol exposure during the first two trimesters-equivalent alters the development of corpus callosum projection neurons in the rat. Alcohol 42:285-93.

Livy DJ, Miller EK, Maier SE, West JR. 2003. Fetal alcohol exposure and temporal vulnerability: Effects of binge-like alcohol exposure on the developing

rat hippocampus. Neurotoxicol and Teratol. 25:447-458.

Lopez-Tejero D, Ferrer I, LLobera M, Herrera E. 1986. Effects of prenatal ethanol exposure on physical growth, sensory reflex maturation and brain development in the rat. Neuropathol Appl Neurobiol. 12(3):251-260.

Lupton C, Burd L, Harwood R. 2004. Cost of fetal alcohol spectrum disorders. American Journal of Medical Genetics Part C (Seminars in Medical Genetics). 127C(1):42-50.

MacLennan AJ, Lee N, Walker DW. 1995. Chronic ethanol administration decreases brain-derived neurotrophic factor gene expression in the rat hippocampus. Neurosci Lett. 197:105–108.

Mallamaci A, Muzio L, Chan CH, Parnavelas J, Boncinelli E. 2000. Area identity shifts in the early cerebral cortex of Emx2-/- mutant mice. Nat Neurosci. 3:679-686.

Mallamaci A, Stoykova A. 2006. Gene networks controlling early cerebral cortex arealization. European Journal of Neuroscience. 23(4):847-856.

Mangale VS, Hirokawa KE, Satyaki PR, Gokulchandran N, Chikbire S, Subramanian L, Shetty AS, Martynoga B, Paul J, Mai MV, Li Y, Flanagan LA, Tole S, Monuki ES. 2008. Lhx2 selector activity specifies cortical identity and suppresses hippocampal organizer fate. Science. 319(5861):304-309.

Mann F, Peuckert C, Dehner F, Zhou R, Bolz J. 2002. Ephrins regulate the formation of terminal axonal arbors during the development of thalamocortical projections. Development. 129:3945-3955.

Marin O, Rubenstein JL. 2003. Cell migration in the forebrain. Annu Rev Neurosci. 26:441-483.

Marjonen H, Sierra A, Nyman A, Rogojin V, Gröhn O, Linden AM, Hautaniemi S, Kaminen-Ahola N. 2015. Early maternal alcohol consumption alters hippocampal DNA methylation, gene expression and volume in a mouse model. PLoS One. 10(5):e0124931.

Maruoka Y, Ohbayashi N, Hoshikawa M, Itoh N, Hogan BL, Furuta. 1998. Comparison of the expression of three highly related genes, Fgf8, Fgf17 and Fgf18, in the mouse embryo. Mechanisms of Development. 74(1-2):175–177.

Mason I. 2007. Initiation to end point: the multiple roles of fibroblast growth factors in neural development. Nat Rev Neurosci. 8:583-596.

Mason JB, Choi SW. 2005. Effects of alcohol on folate metabolism: implications for carcinogenesis. Alcohol. 35:235–241.

Mattson SN, Riley EP, Sowell ER, Jernigan TL, Sobel DF, Jones KL. 1996. A decrease in the size of the basal ganglia in children with fetal alcohol syndrome. Alcohol Clin Exp Res 20:1088-1093.

Mattson SN, Riley EP. 1998. A review of the neurobehavioral deficits in children with fetal alcohol syndrome or prenatal exposure to alcohol. Alcohol Clin Exp Res. 22:279-294.

May PA, Baete A, Russo J, Elliott AJ, Blankenship J, Kalberg WO, Buckley D, Brooks M, Hasken J, Abdul-Rahman O, Adam MP, Robinson LK, Manning M, Hoyme HE. 2014. Prevalence and characteristics of fetal alcohol spectrum disorders. Pediatrics, 134(5), 855-866.

May PA, Gossage JP. 2011. Maternal risk factors for Fetal Alcohol Spectrum Disorders: Not as simple as it might seem. Alcohol Research & Health. 34:15-26.

May PA, Hamrick KJ, Brooke LE, et al. 2004. Nutrition: Its possible contribution to fetal alcohol syndrome among Coloured women in the Western Cape Province of South Africa. Alcohol Clin Exp Res. 28:125A.

May PA, Hamrick KJ, Corbin KD, Hasken JM, Marais AS, Brooke LE, Blankenship J, Hoyme HE, Gossage JP. 2014. Dietary intake, nutrition, and fetal alcohol spectrum disorders in the Western Cape Province of South Africa. Reprod Toxicol 46:31-39.

May PA, Hymbaugh KJ, Aase JM, Samet JM. 1983. Epidemiology of fetal alcohol syndrome among American Indians of the Southwest. Social Biology. 30:374-387.

Mehedindt MG, Craciunescu CN, Zeisel SH. 2010. Maternal dietary choline availability alters angiogenesis in fetal mouse hippocampus. Proc Natl Acad Sci U S A 107:12834–12839.

Mellen M, Ayata P, Dewell S, Kriaucionis S, Heintz N. 2012. MeCP2 binds to 5hmC enriched within active genes and accessible chromatin in the nervous system. Cell. 151(7):1417–30.

Meshorer E. 2007. Chromatin in embryonic stem cell neuronal differentiation. Histol Histopathol. 22:311-319.

Miller MW. 1988. Effect of prenatal exposure to ethanol on the development of cerebral cortex: I. Neuronal generation. Alcohol Clin Exp Res 12:440–449.
Miranda TB, Jones PA. 2007. DNA methylation: the nuts and bolts of repression. J Cell Physiol. 213:384–390.

Miyashita-Lin EM, Hevner R, Wassarman K. Montzka, Martinez S, Rubenstein JLR. 1999. Early Neocortical Regionalization Is Preserved in the Absence of Thalamic Innervation. Science. 285:906-909.

Monuki ES, Porter FD, Walsh CA. 2001. Patterning of the dorsal telencephalon and cerebral cortex by a roof plate-Lhx2 pathway. Neuron. 32:591-604.

Mooney SM, Miller MW. 2010. Prenatal exposure to ethanol affects postnatal neurogenesis in thalamus. Exp Neurol 223:566-73.

Muralidharan P, Sarmah S, Marrs JA. 2015. Zebrafish retinal defects induced by ethanol exposure are rescued by retinoic acid and folic acid supplement. Alcohol. 49(2) 149-163.

Nagarajan RP, Hogart AR, Gwye Y, Martin MR, LaSalle JM. 2006. Reduced MeCP2 expression is frequent in autism frontal cortex and correlates with aberrant MECP2 promoter methylation. Epigenetics. 1(4):e1-11.

Nakagawa Y, Johnson JE, O'Leary DD. 1999. Graded and areal expression patterns of regulatory genes and cadherins in embryonic neocortex independent of thalamocortical input. Journal of Neuroscience. 19:10877-10885.

National Institute on Alcohol Abuse and Alcoholism. 2004. National Institute of Alcohol Abuse and Alcoholism Council approves definition of binge drinking. NIAAA Newsletter.

National Institute on Alcohol Abuse and Alcoholism. 2005. Alcohol: A Women's Health Issue. Bethesda, MD.

Nery S, Fishell G, Corbin JG. 2002. The caudal ganglionic eminence is a source of distinct cortical and subcortical cell populations. Nat Neurosci. 5:1279-1287.

Niccols A. 2007. Fetal alcohol syndrome and the developing socio-emotional brain. Brain Cogn 65:135-142.

Norman AL, Crocker N, Mattson SN, Riley EP. 2009. Neuroimaging and fetal alcohol spectrum disorders. Dev Disabil Res Rev 15:209-217.

Norton JD. 2000. ID helix-loop-helix proteins in cell growth, differentiation and tumorigenesis. Journal of cell science. 113(22), 3897-3905.

Nunez CC, Roussotte F, Sowell ER. 2011. Focus on: structural and functional brain abnormalities in fetal alcohol spectrum disorders. Alcohol Res Health 34:121-131.

O'Leary DD, Sahara S. 2008. Genetic regulation of arealization of the neocortex. Curr Opin Neurobiol. 18:90-100.

O'Leary DD, Chou SJ, Sahara S. 2007. Area patterning of the mammalian cortex. Neuron. 56(2):252-269.

O'Leary DD, Wilkinson DG. 1999. Eph receptors and ephrins in neural development. Curr Opin Neurobiol. 9:65-73.

O'Leary DD. 1989. Do cortical areas emerge from a protocortex? Trends Neurosci. 12:400–406.

O'Leary DDM, Nakagawa Y. 2002. Patterning centers, regulatory genes and extrinsic mechanisms controlling arealization of the neocortex. Curr Opin Neurobiol. 12:14–25.

O'Leary DDM, Sahara S. 2008. Genetic regulation of arealization of the neocortex. Curr Opin Neurobiol. 18(1):90-100.

Ohkubo Y, Chiang C, Rubenstein JL. 2002. Coordinate regulation and synergistic actions of BMP4, SHH and FGF8 in the rostral prosencephalon regulate morphogenesis of the telencephalic and optic vesicles. Neuroscience. 111(1):1-17.

Okada T, Okumura Y, Motoyama J, Ogawa M. 2008. FGF8 signaling patterns the telencephalic midline by regulating putative key factors of midline development. Developmental Biology. 320(1):92-101.

Oladehin A, Margret CP, Maier SE, Li CX, Jan TA, Chappell TD, Waters RS . 2007. Early postnatal alcohol exposure reduced the size of vibrissal barrel field in rat somatosensory cortex (SI) but did not disrupt barrel field organization. Alcohol 41:253–261.

Olino TM, Pettit JW, Klein DN, Allen NB, Seeley JR, Lewinsohn PM. 2008. Influence of parental and grandparental major depressive disorder on behavior

problems in early childhood: a three-generation study. J Am Acad Child Adolesc Psychiatry 47:53–60.

Olson HC, Ohlemiller MM, O'Connor MJ, Brown CW, Morris CA, Damus K, National Task Force on Fetal Alcohol Syndrome and Fetal Alcohol Effect. 2009. A call to action: Advancing Essential Services and Research on Fetal Alcohol Spectrum Disorders - A report of the National Task Force on Fetal Alcohol Syndrome and Fetal Alcohol Effect, March 2009. www.cdc.gov/ncbddd/fas

Panchision DM, Pickel JM, Studer L, Lee SH, Turner PA, Hazel TG, McKay RD. 2001. Sequential actions of BMP receptors control neural precursor cell production and fate. Genes & Development. 15(16):2094–2110.

Pandey SC, Ugale R, Zhang H, Tang L, Prakash A. 2008. Brain chromatin remodeling: a novel mechanism of alcoholism. J Neurosci. 28:3729-3737.

Park HJ, Hong M, Bronson RT, Israel MA, Frankel WN, Yun K. 2013. Elevated Id2 expression results in precocious neural stem cell depletion and abnormal brain development. Stem Cells. 31(5), 1010-1021.

Pasquale EB. Eph receptor signaling casts a wide net on cell behaviour. 2005. Nat Rev Mol Cell Biol. 6:462-475.

Patten AR, Sickmann HM, Dyer RA, Innis SM, Christie BR. 2013. Omega-3 fatty acids can reverse the long-term deficits in hippocampal synaptic plasticity caused by prenatal ethanol exposure. Neuroscience letters. 551:7-11.

Paula-Barbosa MM, Brandaõ F, Madeira MD, Cadete-Leite A. 1993. Structural changes in the hippocampal formation after long-term alcohol consumption and withdrawal in the rat. Addiction 88:237–247.

Petković G, Barisić I. 2010. FAS prevalence in a sample of urban schoolchildren in Croatia. Reproductive Toxicology. 29(2):237-241.

Pfaffl MW. 2001. A new mathematical model for relative quantification in real-time RT-PCR. Nucleic Acids Res. 29, 2002e2007.

Piche M, Chabot N, Bronchti G, Miceli D, Lepore F, Guillemot JP. 2007. Auditory responses in the visual cortex of neonatally enucleated rats. Neuroscience. 145:1144-1156.

Pickering C, Alsiö J, Morud J, Ericson M, Robbins TW, Söderpalm B. 2015. Ethanol impairment of spontaneous alternation behaviour and associated changes in medial prefrontal glutamatergic gene expression precede putative markers of dependence. Pharmacol Biochem Behav. 2;132:63-70.

Pierce DR, West JR. 1986. Blood alcohol concentration: A critical factor for producing fetal alcohol effects. Alcohol. 3:269-272.

Porter FD, Drago J, Xu Y, Cheema SS, Wassif C, Huang SP, Lee E, Grinberg A, Massalas JS, Bodine D, et al. 1997. Lhx2, a LIM homeobox gene, is required for eye, forebrain, and definitive erythrocyte development. Development. 124:2935-2944.

Powrozek TA, Zhou FC. 2005. Effects of prenatal alcohol exposure on the development of the vibrissal somatosensory cortical barrel network. Brain Res Dev Brain Res. 155:135-146.

Puelles L, Kuwana E, Bulfone A, Shimamura K, Keleher J, Smiga S, Puelles E, Rubenstein JLR. 2000. Pallial and subpallial derivatives in the embryonic chick and mouse telencephalon, traced by the expression of the Dlx-2, Emx-1, Nkx-2.1, Pax-6 and Tbr-1 genes. Journal of Comparative Neurology. 424:409-438.

Ragsdale CW, Grove EA. 2001. Patterning the mammalian cerebral cortex. Curr Opin Neurobiol. 11:50-58.

Rakic P, Ayoub AE, Breunig JJ, Dominguez MH .2009. Decision by division: making cortical maps. Trends Neurosci. 32:291-301.

Rakic P, Suner I, Williams RW .1991. A novel cytoarchitectonic area induced experimentally within the primate visual cortex. Proc Natl Acad Sci U S A. 88:2083–2087.

Rakic P. 1988. Specification of cerebral cortical areas. Science. 241:170-176. Rallu M, Corbin JG, Fishell G. 2002. Parsing the prosencephalon. Nat Rev Neurosci. 3:943–951.

Rash BG, Grove EA. 2006. Area and layer patterning in the developing cerebral cortex. Curr Opin Neurobiol. 16:25–34.

Rash BG, Grove EA. 2007. Patterning the dorsal telencephalon: a role for sonic hedgehog? J Neurosci. 27:11595-11603.

Rauschecker JP, Henning P. 2001. Crossmodal expansion of cortical maps in early blindness. In: Kaas J, editor. The mutable brain. Amsterdam (the Netherlands): Gordon and Breach Publishing Group. p. 243-259.

Rauschecker JP, Korte M. 1993. Auditory compensation for early blindness in cat cerebral cortex. J Neurosci. 13:4538--4548.

Renthal W, Nestler EJ. 2009. Chromatin regulation in drug addiction and depression. Dialog Clin. Neurosci. 11, 257–268.

Rice FL, Van der Loos H. 1977. Development of the barrels and barrel field in the somatosensory cortex of the mouse. J Comp Neurol. 171:545-560.

Riggs AD. Pfeifer GP 1992. X-chromosome inactivation and cell memory. Trends Genet. 8:169–174.

Riikonen RS, Salonen I, Partanen K, Verho S. 1999. Brain perfusion SPECT and MRI in fetal alcohol syndrome. Dev Med Child Neurol 41:652-659.

Rubenstein JLR, Anderson S, Shi L, Miyashita-Lin E, Bulfone A, Hevner R. 1999. Genetic control of cortical regionalization and connectivity. Cereb Cortex. 9:524-532.

Rubenstein JLR. Development of the Cerebral Cortex: Implications for Neurodevelopmental Disorders. 2011. J Child Psychol Psychiatry. 52(4):339-355.

Rustay NR, Wahlsten D, Crabbe JC. 2003. Influence of task parameters on rotarod performance and sensitivity to ethanol in mice. Behav Brain Res. 141:237-249.

Sansom SN, Livesey FJ. 2009. Gradients in the brain: the control of the development of form and function in the cerebral cortex. Cold Spring Harb Perspect Biol. 1(2):a002519.

Schaeren-Wiemers N, Andre E, Kapfhammer JP, Becker-Andre M. 1997. The expression pattern of the orphan nuclear receptor RORbeta in the developing and adult rat nervous system suggests a role in the processing of sensory information and in circadian rhythm. Eur J Neurosci. 9:2687-2701.

Schlaggar BL, O'Leary DD .1991. Potential of visual cortex to develop an array of functional units unique to somatosensory cortex. Science. 252:1556-1560.

Seelke AMH, Dooley JC, Krubitzer LA. 2012. The Emergence of Somatotopic Maps of the Body in S1 in Rats: The Correspondence Between Functional and Anatomical Organization. PLoS ONE. 7(2): e32322.

Shaw P, Kabani NJ, Lerch JP, Eckstrand K, Lenroot R, Gogtay N, Greenstein D, Clasen L, Evans A, Rapoport JL, Giedd JN, Wise SP. 2008. Neurodevelopmental trajectories of the human cerebral cortex. J Neurosci 28(14):3586-3594.

Sheleg M, Yochum CL, Wagner GC, Zhou R, Richardson JR. 2013. Ephrin-A5 deficiency alters sensorimotor and monoaminergic development. Behav Brain Res. 236:139-147.

Shimamura K, Rubenstein JL. 1997. Inductive interactions direct early regionalization of the mouse forebrain. Development. 124(14):2709-2718.

Shimogori T, Banuchi V, Ng HY, Strauss JB, Grove EA. 2004. Embryonic signaling centers expressing BMP, WNT and FGF proteins interact to pattern the cerebral cortex. Development. 131:5639-5647.

Shimogori T, Grove EA. 2005. Fibroblast growth factor 8 regulates neocortical guidance of area-specific thalamic innervation. J Neurosci. 25(28):6550-6560.

Smith MM. 1991. Histone structure and function. Curr Opin Cell Biol. 3:429-437.

Smith SS, Kaplan BE, Sowers LC, Newman EM. 1992. Mechanism of human methyl-directed DNA methyltransferase and the fidelity of cytosine methylation. Proc Natl Acad Sci U S A. 89(10):4744-4748.

Smith ZD, Meissner A. 2013. DNA methylation: roles in mammalian development. Nat Rev Genet. 14(3):204–20.

Sokol RJ, Delaney-Black V, Nordstrom B. 2003. Fetal alcohol spectrum disorder. JAMA. 290:2996–2999.

Sowell ER, Thompson PM, Leonard CM, Welcome SE, Kan E, Toga AW. 2004. Longitudinal mapping of cortical thickness and brain growth in normal children. J Neurosci 24:8223–8231.

Sowell ER, Thompson PM, Mattson SN, Tessner KD, Jernigan TL, Riley EP, Toga AW. 2002a. Regional brain shape abnormalities persist into adolescence after heavy prenatal alcohol exposure. Cereb Cortex 12:856-865.

Sowell ER, Thompson PM, Peterson BS, Mattson SN, Welcome SE, Henkenius AL, Riley EP, Jernigan TL, Toga AW. 2002b. Mapping cortical gray matter asymmetry patterns in adolescents with heavy prenatal alcohol exposure. Neuroimage 17:1807-1819.

Stade B, Ali A, Bennett D, Campbell D, Johnston M, Lens C, et al. 2009. The burden of prenatal exposure to alcohol: revised measurement of cost. Canadian Journal of Clinical Pharmacolology. 16(1):e91-e102.

Stenkamp DL, Kashyap B, Sloan B. 2009. Ethanol-Induced Microphthalmia in the Zebrafish Embryo is not Mediated by the Retinoic Acid or Hedgehog Signaling Pathways. Invest Ophth Vis Sci. (50)13:1298-1298.

Storm EE, Garel S, Borello U, Hebert JM, Martinez S, McConnell SK, Martin GR, Rubenstein JLR. 2006. Dose-dependent functions of Fgf8 in regulating telencephalic patterning centers. Development. 133:1831-1844.

Strahl BD, Allis CD. 2000. The language of covalent histone modifications. Nature. 403:41-45.

Stratton K, Howe C, Battaglia F. 1996. Institute of Medicine. Fetal Alcohol Syndrome: Diagnosis, Epidemiology, Prevention, and Treatment. Washington, DC; National Academy Press.

Streissguth AP, Barr HM, Martin DC. 1984. Alcohol exposure in utero and functional deficits in children during the first four years of life. Ciba Found Symp. 105:176-196.

Sulik KK, Johnston MC, Andwebb MA. 1981. Fetal alcohol syndrome: Embryogenesis in a mouse model. Science. 214:936-938.

Sulik KK. 2005. Genesis of alcohol-induced craniofacial dysmorphism. Exp Biol Med. 230:366-75.

Sur M, Rubenstein JL. 2005. Patterning and plasticity of the cerebral cortex. Science. 310:805–810.

Surani MA, Hayashi K, Hajkova P. 2007. Genetic and epigenetic regulators of pluripotency. Cell. 128:747-762.

Suzuki SC, Inoue T, Kimura Y, Tanaka T, Takeichi M. 1997. Neuronal circuits are subdivided by differential expression of type-II classic cadherins in postnatal mouse brains. Mol Cell Neurosci. 9:433-447.

Szulwach KE, Li X, Li Y, Song CX, Wu H, Dai Q, et al. 2011. 5-hmC-mediated epigenetic dynamics during postnatal neurodevelopment and aging. Nat Neurosci. 14(12):1607–16.

Takai D, Jones PA. 2002. Comprehensive analysis of CpG islands in human chromosomes 21 and 22. Proc Natl Acad Sci USA. 99:3740-3745.

Tamnes CK, Ostby Y, Fjell AM, Westlye LT, Due-Tonnessen P, Walhovd KB. 2010. Brain maturation in adolescence and young adulthood: Regional age-related changes in cortical thickness and white matter volume and microstructure. Cereb Cortex 20:534–548.

Tamura T, Goldenberg RL, Johnston KE, Chapman VR. 2004. Relationship between prepregnancy BMI and plasma zinc concentrations in early pregnancy. Brit J Nutr. 91:773-777.

Tarelo-Acuna L, Olvera-Cortes ME, Gonzalez-Burgos I. 2000. Prenatal and postnatal exposure to ethanol induces changes in the shape of the dendritic spines from hippocampal CA1 pyramidal neurons of the rat. Neuroscience Letters 286:13–16.

Tenkova T, Young C, Dikranian K, Labruyere J, Olney JW. 2003. Ethanol-induced apoptosis in the developing visual system during synaptogenesis. Invest Ophth Vis Sci. 44(7), 2809-2817.

Theil T, Dominguez-Frutos E, Schimmang T. 2008. Differential requirements for Fgf3 and Fgf8 during mouse forebrain development. Developmental Dynamics. 237(11):3417-3423.

Thomas JD, Biane JS, O'Bryan KA, O'Neill TM, Dominguez HD. 2007. Choline supplementation following third-trimester equivalent alcohol exposure attenuates behavioral alterations in rats. Behav Neurosci. 121:120-130.

Thomas JD, Idrus NM, Monk BR, Dominquez HD. 2010. Prenatal choline supplementation mitigates behavioral alterations associated with prenatal alcohol exposure in rats. Birth Defects Res A Clin Mol Teratol. 88:827-837.

Tissir F, Goffinet AM. 2003. Reelin and brain development. Nat Rev Neurosci. 4:496-505.

Treit S, Zhou D, Lebel C, Rasmussen C, Andrew G, Beaulieu C. 2014. Longitudinal MRI reveals impaired cortical thinning in children and adolescents prenatally exposed to alcohol. Human brain mapping. 35(9) 4892-4903.

Tsankova N, Renthal W, Kumar A, Nestler EJ. 2007. Epigenetic regulation in psychiatric disorders. Nat Rev Neurosci. 8:355-367.

Tunc-Ozcan E, Ullmann TM, Shukla PK, Redei EE. 2013. Low-Dose Thyroxine Attenuates Autism-Associated Adverse Effects of Fetal Alcohol in Male Offspring's Social Behavior and Hippocampal Gene Expression. Alcohol Clin Exp Res. 37(11):1986-1995.

Urban M, Chersich MF, Fourie LA, Chetty C, Olivier L, Viljoen D. 2008. Fetal alcohol syndrome among grade 1 schoolchildren in Northern Cape Province: Prevalence and risk factors. S Afr Med J. 98:877-882.

Uzinova MB, Benezra R. 2003. Id proteins in development, cell cycle and cancer. Trends Cell Biol. 13(8), 410-8.

Van der Loos H, Dorfl J, Welker E. 1984. Variation in pattern of mystacial vibrissae in mice. A quantitative study of ICR stock and several inbred strains. J Hered. 75:326-336.

Van der Loos H, Dorfl J. 1978. Does the skin tell the somatosensory cortex how to construct a map of the periphery? Neurosci Lett. 7:23-30.

Van der Loos H, Welker E, Dorfl J, Rumo G. 1986. Selective breeding for variations in patterns of mystacial vibrissae of mice. Bilaterally symmetrical strains derived from ICR stock. J Hered. 77:66-82.

Van der Loos H, Woolsey TA. 1973. Somatosensory cortex: structural alterations following early injury to sense organs. Science. 179:395-398.

van Holde KE. 1988. Chromatin (ed. Rich, A.) 1–148 (Springer, New York). Vanderhaeghen P, Lu Q, Prakash N, Frisen J, Walsh CA, Frostig RD, Flanagan JG. 2000. A mapping label required for normal scale of body representation in the cortex. Nat Neurosci. 3:358-365.

Vernescu RM, Adams RJ, Courage ML. 2012. Children with fetal alcohol spectrum disorder show an amblyopia-like pattern of vision deficit. Dev Med Child Neurol 54:557-62.

Vue TY, Lee M, Tan YE, Werkhoven Z, Wang L, Nakagawa Y. 2013. Thalamic control of neocortical area formation in mice. J Neurosci. 33(19):8442-8453.

Welker C. 1971. Microelectrode delineation of fine grain somatotopic organization of (SmI) cerebral neocortex in albino rat. Brain Research. 26:259-275.

Welker E, Van der Loos H. 1986. Quantitative correlation between barrel-field size and the sensory innervation on the whiskerpad: A comparative study in six strains of mice bred for different patterns of mystacial vibrissae. J Neurosci. 6:3355-3373.

West JR, Goodlett CR. 1990. Teratogenic effects of alcohol on brain development. Annals of Medicine. 22:319-325.

Willford JA, Chandler LS, Goldschmidt L, Day NL. 2010. Effects of prenatal tobacco, alcohol and marijuana exposure on processing speed, visual–motor coordination, and interhemispheric transfer. Neurotoxicology and teratology, 32(6), 580-588.

Willford JA, Richardson GA, Leech SL, Day N. 2004. Verbal and visuospatial learning and memory function in children with moderate prenatal alcohol exposure. Alcohol Clin Exp Res 28:497–507.

Willoughby KA, Sheard ED, Nash K, Rovet J. 2008. Effects of prenatal alcohol exposure on hippocampal volume, verbal learning, and verbal and spatial recall in late childhood. J Int Neuropsychol Soc 14:1022-1033.

Wise SP, Jones EG .1978. Developmental studies of thalamocortical and commissural connections in the rat somatic sensory cortex. J Comp Neurol. 178:187–208.

Wong-Riley M, Carroll EW. 1984. Effect of impulse blockage on cytochrome oxidase activity in monkey visual system. Nature. 307(5948):262-264.

Woods KJ, Meintjes EM, Molteno CD, Jacobson SW, Jacobson JL. 2015. Parietal dysfunction during number processing in children with fetal alcohol spectrum disorders. Neuroimage Clin. 8:594-605.

Woolsey TA, Van der Loos H. 1970. The structural organization of layer IV in the somatosensory region (SI) of mouse cerebral cortex. The description of a cortical field composed of discrete cytoarchitectonic units. Brain Research. 17:205-242.

Woolsey TA, Welker C, Schwartz RH. 1975. Comparative anatomical studies of the SmI face cortex in special reference to the barrels. Journal of Comparative Neurology. 164:79-94.

Wozniak JR, Mueller BA, Bell CJ, Muetzel RL, Hoecker HL, Boys CJ, Lim KO. 2013. Global functional connectivity abnormalities in children with fetal alcohol spectrum disorders. Alcohol Clin Exp Res. 37(5):748-56.

Xie N, Yang Q, Chappell TD, Li CX, Waters RS. 2010. Prenatal alcohol exposure reduces the size of the forelimb representation in motor cortex in rat: an intracortical microstimulation (ICMS) mapping study. Alcohol. 44(2):185-94.

Xu WS, Parmigiani RB, Marks PA. 2007. Histone deacetylase inhibitors: molecular mechanisms of action. Oncogene. 26:5541-5552.

Yang Y, Roussotte F, Kan E, Sulik KK, Mattson SN, Riley EP, Jones KL, Adnams CM, May PA, O'Connor MJ, Narr KL, Sowell ER. 2011. Abnormal cortical thickness alterations in fetal alcohol spectrum disorders and their relationships with facial dysmorphology. Cereb Cortex 22:1170-1179.

Ye W, Shimamura K, Rubenstein JL, Hynes MA, Rosenthal A. 1998. FGF and Shh signals control dopaminergic and serotonergic cell fate in the anterior neural plate. Cell. 93(5):755–766.

Yokota Y, Mori S. 2002. Role of Id family proteins in growth control. J. Cell. Physiol. 190, 21-28.

Yun ME, Johnson RR, Antic A, Donoghue MJ. 2003. EphA family gene expression in the developing mouse neocortex: regional patterns reveal intrinsic programs and extrinsic influence. J Comp Neurol. 456:203-216.

Zhang LI, Bao S, Merzenich MM. 2002. Disruption of primary auditory cortex by synchronous auditory inputs during a critical period. Proc Natl Acad Sci USA. 99:2309-2314.

Zhao X, Pak C, Smrt RD, Jin P. 2007. Epigenetics and Neural developmental disorders: Washington DC, September 18 and 19, 2006. Epigenetics. 2:126-134.

Zhou C, Tsai SY, Tsai MJ. 2001. COUP-TFI: an intrinsic factor for early regionalization of the neocortex. Genes Dev. 15:2054-2059.

Zhou D, Lebel C, Lepage C, Rasmussen C, Evans A, Wyper K, Pei J, Andrew G, Massey A, Massey D, Beaulieu C. 2011. Developmental cortical thinning in fetal alcohol spectrum disorders. Neuroimage 58:16–25.

Zhou FC, Sari Y, Zhang JK, Goodlett CR, Li T. 2001. Prenatal alcohol exposure retards the migration and development of serotonin neurons in fetal C57BL mice. Brain Res Dev Brain Res. 126:147-155.